EXPERIMENTS ON THE TRANSPORTATION OF SUSPENDED SEDIMENT BY WATER

Thesis by

Vito A. Vanoni

In Partial Fulfillment of the Requirements for the Degree of
Doctor of Philosophy, California Institute of Technology,
Pasadena, California

1940

UNITED STATES DEPARTMENT OF AGRICULTURE
Soil Conservation Service
Washington, D. C.
H. H. Bennett, Chief

EXPERIMENTS ON THE TRANSPORTATION OF SUSPENDED SEDIMENT BY WATER

Vito A. Vanoni

Sedimentation Studies Division, Soil Conservation Service

Cooperative Laboratory
California Institute of Technology
Pasadena, California

May 1940

TABLE OF CONTENTS

SUMMARY

Measurements of the sediment and velocity distributions in a laboratory flume were made for various values of rate of flow, slope of channel, and size and amount of suspended load. The experimental sediment-distribution measurements were compared with the theoretical distribution which assumes that the coefficient for the turbulent transfer of suspended sediment is the same as the coefficient for the turbulent transfer of momentum.

The following are the main findings:

(1) The measured sediment distributions have the same form as the theoretical distribution but do not agree quantitatively with them, thus showing, as was anticipated, the invalidity of the assumption that the transfer coefficient for sediment was equal to that for momentum. In general the measurements gave larger concentrations than the theory when the suspended load was fine, while as the size of the sediment was increased the agreement improved up to a certain size of sediment beyond which the tendency was in the opposite direction.

(2) Suspended sediment in a flow tends to reduce appreciably the turbulent transfer of momentum and hence the resistance to flow, allowing the sediment-laden water to flow more rapidly than a comparable clear water flow. This effect increases with the total sediment load and with a decrease in the grain size of the sediment.

(3) Suspended load in a flow tends to produce instability and may be a factor in causing the secondary circulation observed in rivers.

EXPERIMENTS ON THE TRANSPORTATION OF SUSPENDED SEDIMENT BY WATER

Introduction

Many important practical problems of today involve the movement of sediments by water and their complete solution requires more knowledge of this subject than now exists. Flood control and channel maintenance on streams, both large and small, is just as much a problem of sediment movement as it is one of flow of water. As a matter of fact established practices are quite successful in handling the water flow of floods but the problem of passing the sediment load is still unsolved. The work of the United States Department of Agriculture in recent years in developing methods of reducing accelerated erosion on agricultural lands has encountered many new sediment-transportation problems that have shown the urgent need for additional fundamental knowledge of this subject. It is in connection with these latter needs that this study was undertaken.

Sediment may be transported by flowing water in essentially two different ways, i.e., by rolling or sliding along the bed of the stream channel or in suspension in the body of the fluid. Material transported by the former method is called the bedload of the stream, or simply bedload, while that carried in the latter way is called the suspended load. In the neighborhood of the bed a continual interchange of material is occurring between the bed and the overlying fluid and at this point it is obviously difficult to distinguish between the bedload and suspended load. The two types of transportation are by no means independent, but they are

separated only for convenience in studying and referring to them.

The present study deals only with suspended load. However, before proceeding to the discussion of the main subject a few remarks regarding the relative status of the knowledge of the two kinds of sediment transportation appear to be in order. By far most of the experimental work on sediment transportation has been done on bed load, yet no satisfactory theory for this type of movement has appeared. On the other hand, in the case of suspended load, the theoretical work is far in advance of the experimental, there being no complete experimental data on this phase of transportation. There is an abundance of measurements of suspended load in natural streams, but in general these were made only to estimate the sediment load and consequently do not include all the data necessary to check the theory. Bed-load measurements in natural streams are very few. This may be accounted for, at least in part, by the difficulties and expense of making bed-load measurements just as the ease with which suspended-load measurements can be made, accounts for their relative abundance.

Previous Work

Empirical theories.

Among the earliest suspended-load transportation studies were those made by British engineers on the irrigation systems in India. The problem here was to design canals so that sediment in the waters diverted from rivers would not be deposited, while at the same time no erosion of the boundaries of the canals would occur. Kennedy (1) made a study of

this problem upon which he based an empirical expression for the equilibrium velocity that would neither deposit or remove material. His expression which was proposed in 1895, was of the form

$$V = c\, d^{n} \qquad (1)$$

where V is the equilibrium velocity, d is the mean depth and c and n are constants. For the Indian canals and the foot-second system of units, Kennedy obtained values of 0.84 and 0.64 respectively, for c and n. He expected c to vary with the grain size of the sediment load but did not feel that n would vary appreciably.

Attempts to apply relations of this type to similar problems in this country (2) have met with only partial success since conditions were apparently different from those upon which the relation was based. Other engineers have varied the constants c and n in the Kennedy formula in an attempt to make it cover a wider range of conditions but no attempts to introduce other variables seem to have been made.

Griffiths (3) developed an expression for the silt load of a stream by assuming that in the empirical Kennedy formula V is the average velocity in a vertical of the cross-section, d is the depth at this point and c is a coefficient proportional to the sediment load G_1 in parts per 10,000 by weight.

$$G_1 = c_1\, c \qquad (2)$$

Eliminating c from 1 and 2, and rearranging

$$G_1 = c_1 \frac{V}{d^{n}} \qquad (3)$$

By fitting the expression (3) to measured data Griffiths obtained

values of 7.5 for c_1 and 0.57 for n. Engineers discussing (3) his work pointed out that the expression failed to account for all of the variables affecting sediment transportation and could not apply generally. Despite the empirical nature of the formula in some cases it appears to give results that are satisfactory.

Students of sediment transportation recognized that turbulence was a major factor in keeping the material in suspension and attempted to develop expressions for the vertical components of the turbulence. Once the vertical turbulence velocity was known it would be possible to determine the maximum size of material that could be supported, and therefore, transported. Among these attempts was that of Krey (4) who assumed that the distribution of vertical velocity was elliptical with the maximum at mid-depth. This assumption is to be questioned since measurements (5) have shown that the turbulence is a maximum at the boundary of the channel and diminishes with the distance from the boundary.

Modern theories.

Modern theories of suspended-load transportation are based upon the developments in the mechanics of turbulent flow of fluids.

Consider a two-dimensional turbulent flow in the x direction with a velocity U(y), where y is normal to x. Then according to Reynolds (6) the shear parallel to x, on a plane normal to y may be expressed by

$$\tau = -\rho \overline{U' V'} \qquad (4)$$

where ρ is the mass density of the fluid and U' and V' are the turbulent velocity fluctuations in the x and y directions respectively, and the

bar denotes mean value. Although this result was originally obtained by applying the Navier-Stokes equations, as shown by Prandtl (7) it may also be obtained by a direct application of the momentum theorum.

Equation (4) is of value in explaining the existence of the turbulent shear stress but before it can be used practically it must be possible to express the mean product in terms of known flow characteristics. Boussinesq (8) introduced an expression for the shear of the form,

$$\tau = \rho \epsilon \frac{dU}{dy} \qquad (5)$$

where the quantity $\rho\epsilon$ is analogous to the coefficient of viscosity in the expression for viscous shear and U is the mean velocity in the x direction. The quantity ϵ has the dimension of a kinematic viscosity but unlike its counterpart it is a function of flow conditions, and therefore, varies from point to point.

Equation (5) may be written in the form,

$$\tau = \epsilon \frac{d}{dy} (\rho U) \qquad (6)$$

The term $\frac{d}{dy}(\rho U)$ is the momentum gradient in the y direction, and since the shear stress is equal to the momentum transferred through unit area in unit time, the quantity ϵ is a coefficient expressing the exchange of fluid between neighboring filaments. This quantity is called the coefficient of turbulent exchange. Obviously it has the dimensions, length x velocity.

In order to proceed beyond the work of Boussinesq, Prandtl introduced into turbulence theory the concept of the "mixing length" which is

analogous to the "mean free path" in the kinetic theory of gases. According to this concept the fluctuation U' is put equal to the mixing length ℓ times the mean velocity gradient $\frac{dU}{dy}$ and V' is assumed proportional to U' or,

$$U' = \ell \frac{dU}{dy} \tag{7}$$

and

$$V' \sim U' \tag{8}$$

Introducing equations (7) and (8) into equation (4) and absorbing the constant of proportionality in ℓ,

$$\tau = \rho \ell^2 \left(\frac{dU}{dy}\right)^2 \tag{9}$$

The correlation coefficient β_1, between the velocity fluctuations U' and V' is defined by,

$$\beta_1 = \frac{\overline{U'V'}}{\sqrt{\overline{U'^2}}\sqrt{\overline{V'^2}}} \tag{10}$$

Introducing equations (7) and (10) into (4), there is obtained,

$$\tau = \beta_1 \rho \sqrt{\overline{V'^2}}\, \ell \frac{dU}{dy} \tag{11}$$

von Kármán (11) defines a correlation coefficient β such that

$$\tau = \beta \rho V' \ell \frac{dU}{dy} \tag{12}$$

where V' is the average of the absolute values of the fluctuations normal to the main flow. From equation (12) it is seen that the coefficient of turbulent mixing ϵ, has the value,

$$\epsilon = \beta V' \ell \tag{13}$$

and the dimensions, velocity x length.

Just as equation (12) expresses the rate of transfer of momentum due to turbulent mixing, it is possible to write by a similar equation the transfer of heat, suspended particles or any other property that is carried by the fluid. Thus, the turbulent heat transfer in unit area and time is

$$g_h = -\beta c_s \, v' \ell \frac{d\theta}{dy} \tag{14}$$

and the rate of transfer of mass of suspended particles per unit area is

$$G = -\beta \, v' \ell \frac{dC}{dy} \tag{15}$$

where c_s is the specific heat of the fluid, θ the temperature, and C the concentration of suspended material in mass per unit volume. von Kármán (11) pointed out that the values of β, v' and ℓ in equation (12), (14), and (15) need not necessarily be the same.

It is interesting to note that transfer occurs only when there is a gradient of the property being transferred and that the net transfer is in the direction of decreasing concentration. If, for instance, in a suspension of particles there is no gradient the particles are uniformly distributed in the fluid, and turbulent mixing will merely result in a circulation of the material. On the other hand, when there is a mixing between levels of different concentration the less laden fluid is exchanged for fluid containing more particles and the result tends toward a more uniform distribution of the suspended material.

For steady conditions in a suspension of particles, such as occurs in suspended-sediment transportation, the turbulent transfer of particles in the upward direction is balanced by the settling of the particles due to the force of gravity or,

$$-\beta \, v' \ell \frac{dC}{dy} = wC \tag{16}$$

where w is the settling velocity of the particles in the undisturbed fluid. Transposing and introducing equation (13) the differential equation for suspended sediment becomes,

$$wC + \epsilon \frac{dC}{dy} = 0 \qquad (17)$$

Solution of equation (17) gives,

$$\log_e \frac{C}{C_a} = - w \int_a^y \frac{dy}{\epsilon} \qquad (18)$$

where C_a is the concentration at an arbitrary reference level $y = a$.

If ϵ is constant over the depth, i.e., $\epsilon (y) =$ constant, equation (18) may be integrated to give,

$$\frac{C}{C_a} = e^{- \frac{w}{\epsilon} (y-a)} \qquad (19)$$

where e is the base of the natural logarithms.

The above relation was apparently first given by Schmidt (12) who applied it to the study of suspension of dust particles in the atmosphere. Equation (17) was derived by a formal procedure by O'Brien (13). The more direct derivation given above is due to von Kármán (11).

In general $\epsilon = \rho v' l$ is a function of y and must be so expressed before equation (18) can be solved. Such a relation is furnished by the momentum-transfer theory, i.e., equations (5) or (12), which yields the expression for the coefficient of turbulent exchanges as follows,

$$\epsilon = \rho v' l = \frac{\tau}{\rho \frac{dU}{dy}} \qquad (20)$$

Introducing equation (20) into equation (18) yields the relation

$$\log_e \frac{C}{C_a} = - \rho w \int_a^y \frac{\frac{dU}{dy}}{\tau} dy . \qquad (21)$$

which was first presented by von Kármán (11) in 1934.

In a uniform open-channel flow whose ratio of width to depth is large, the above relations will apply and in addition the shear stress τ, can be calculated from the slope of the channel. In figure 1 consider the equilibrium of a prism of fluid of unit width and length and of height $d - y$. Summing up the forces in the direction of flow, and noting that the static-pressure forces F, are equal,

$$\tau = \gamma (d - y) S \qquad (22)$$

where γ is the specific weight of the fluid and S is the slope of the channel. The expression can also be written in terms of the shear at the

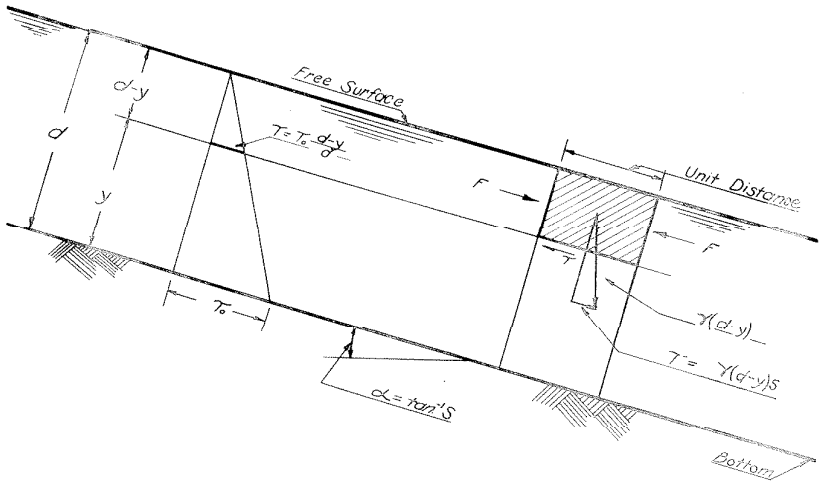

Fig. 1. Calculation of fluid shear in uniform two-dimensional open-channel flow.

boundary as follows:

$$\tau = \tau_0 \frac{d - y}{d} \qquad (23)$$

where τ_0 is the shear at the bottom or from equation (22) $\tau_0 = \gamma d S$.

Note:

The average bottom shear may be calculated by considering the equilibrium of a unit length of the entire cross-section of the stream. The

force acting along the bed is given by $\gamma A S$ where A is the area of cross-section. This is resisted by an average shear $\overline{\tau}_o$, acting over the wetted perimeter of length p, of the channel or

$$\overline{\tau}_o = \frac{\gamma A S}{p} = \gamma R S \qquad (24)$$

where R is the hydraulic radius of the channel. Obviously for wide channels $R = d$ and $\overline{\tau} = \gamma d S$. Equation (24) is named after DuBois (16) and has been used extensively in the development of expressions for bed-load transportation.

Introducing equation (23) into equation (21) there results,

$$\log_e \frac{C}{C_a} = \frac{w}{\frac{\tau_o}{\rho}} \int_a^y \frac{\frac{dU}{dy}}{\frac{d-y}{d}} dy \qquad (25)$$

By computing $\frac{dU}{dy}$ from measured velocities, the distribution of sediment can be calculated from equation (25) for different sediment fractions and compared with actual measurements.

Were it possible to obtain an expression for the velocity gradient the above integral could be evaluated and the distribution of sediment of different grade sizes, i.e., settling velocities, determined from easily obtained flow characteristics. The von Kármán (17) universal velocity defect law,

$$\frac{U - U_{max}}{\sqrt{\frac{\tau_o}{\rho}}} = \frac{1}{k} \log_e \frac{y}{r_o} \qquad (26)$$

has been shown by Nikuradse (18) and (19) to apply to pipes and by Keulegan (20) to also apply to open channels ~~(20)~~ and therefore, furnishes a relation for the velocity distribution. In the equation k is a universal constant (0.40 for pipes), y is the distance from the wall of the pipe of radius r_o. For wide open-channels, as discussed here, r_o in equation (26) is replaced with d, the depth of the flow. The derivative of the velocity then becomes,

$$\frac{dU}{dy} = \frac{1}{k}\sqrt{\frac{\tau_o}{\rho}}\ \frac{1}{y} \tag{27}$$

which, when introduced into equation (25), gives,

$$\log \frac{c}{c_a} = -\frac{w}{k\sqrt{\frac{\tau_o}{\rho}}} \int_a^y \frac{dy}{y\left(\frac{d-y}{d}\right)} \tag{28}$$

Integrating the above expression gives

$$\frac{c}{c_a} = \left[\frac{d-y}{y} \times \frac{a}{d-a}\right]^z = F^z \tag{29}$$

where $z = \dfrac{w}{k\sqrt{\frac{\tau_o}{\rho}}}$. From this equation it is possible to plot the curves

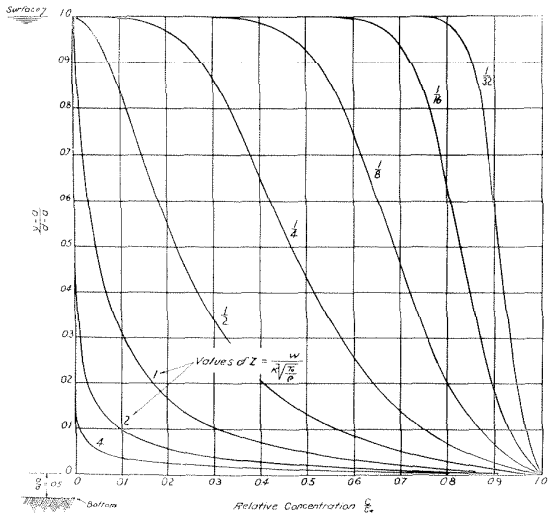

Fig. 2. Distribution of suspended load according to equation 29.

of relative sediment distribution shown in figure 2. This chart was first constructed by Arthur T. Ippen at the suggestion of Professor von Kármán and published by Rouse (21).

It is to be noted that equation (29) as well as those preceding

it give only a relative concentration and therefore, do not make possible the calculation of the total transport of the stream. In order to make this possible a value for C_a is needed and the problem of obtaining the transporting capacity of a flow may be simply stated as one of determining this value. Some attempts have been made to develop relations for total load but this work has not proceeded far enough to indicate its validity. In discussing the magnitude of C_a, von Kármán (11) states that it depends probably on the size of the sediment and on the magnitude of the shearing stress acting at the ground. Rouse (22) has suggested that the limiting value of a in equation (29) be made equal to k_s, the height of the roughness elements. He further suggests that the corresponding concentration C_k, for this level be calculated from equation (19) assuming that in the interval $y = 0$ to $y = k$, $\epsilon(y) = \epsilon(k) = \text{Constant}$, and that the concentration at $y = 0$ be set equal to that of the bed material. Lane and Kalinske (23) approaching the problem from a statistical point of view argue that only those particles having fall velocities w, less than the vertical fluctuations V', of the bed velocity will be picked up. By assuming a normal distribution of V' and setting the root mean-square fluctuation $\sqrt{\overline{V'^2}}$ proportional to the friction velocity $\sqrt{\frac{\tau_o}{\rho}}$ they proceed to calculate the probable rate of suspension of material. As a result of an analyses of the energy balance of suspended-load transportation, Knapp (24) advanced the hypothesis that the capacity of a stream was limited only if the settling velocity w, of the sediment is greater than the rate of fall of the stream $U S$, where U is the average velocity of flow and S is the slope of the channel. When the

settling velocity is less than U_* the material contributes energy to the flow thus making it possible to pick up additional load until extremely high concentrations are reached.

Verification of theories.

Although no comprehensive suspended-load experiments have been made in which the important variables have been systematically investigated, some noteworthy experimental work has been done.

Schmidt (12) appears to have first applied the turbulence theory to the problem of suspended load in his studies of the suspension of dust particles in air. He obtained equation (19) which assumes a constant value for the exchange coefficient.

In 1929 Hurst (25) reported a series of experiments on the suspension of sediment in a cylindrical column of water agitated uniformly by a series of propellers much as was used by Joule in his experiments on the mechanical equivalent of heat. He measured the concentrations at various levels in his apparatus of three well graded sands (mean size 0.9 mm, 0.4 mm, and 0.2 mm) for several propeller speeds and found that the distribution of sediment followed an exponential relationship of the form of equation (19). Hurst was also able to derive his relationship from an analysis based upon the kinetic theory of gases. He considered the vertical equilibrium of a prism of fluid of height dy, having ends of unit area, by treating the particles as molecules in a gravitational field. The pressure on the lower face of the prism is then $1/3\ m\ n\ \overline{v^2}$ where m is the mass of each sand particle, n is the number per unit volume and $\overline{v^2}$ is the mean square of the vertical velocity of the particles. Similar-

ly, the pressure on the upper face is then $1/3\ m\ n\ (n + d\ n)\ \overline{V^2}$ and the effective weight of the particles in the prism is $m\ n\ dy\ g\ \frac{\rho_s - \rho}{\rho_s}$ where ρ_s, and ρ are the densities of the sediment and fluid respectively. Or writing the equilibrium in the vertical direction

$$1/3\ m\ n\ \overline{V^2} - 1/3\ m\ (n + d\ n)\ \overline{V^2} - m\ n\ dy\ \frac{\rho_s - \rho}{\rho_s}\ g = 0$$

$$1/3\ dn\ \overline{V^2} + \frac{\rho_s - \rho}{\rho_s}\ g\ n\ dy = 0$$

solution of which gives Hurst's equation

$$n = n_o\ e^{-\frac{\rho_s - \rho}{\rho_s}\ \frac{3g}{V^2}\ y} \qquad (30)$$

Rouse (26) performed some experiments similar to Hurst's, using an agitator of coarse mesh bars which was oscillated in the vertical direction with simple harmonic motion. The results of this work for a composite sand

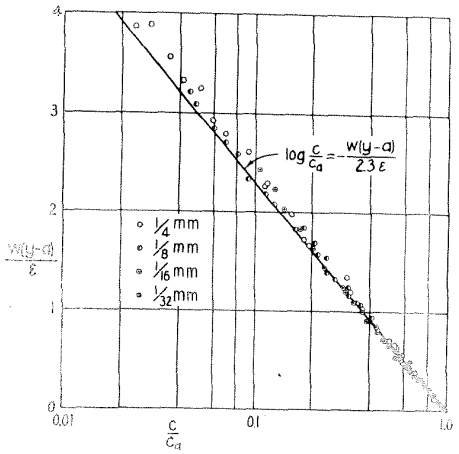

Fig. 3. Vertical Distribution of the components of a sediment mixture for conditions of uniform turbulence. (Rouse)

shown in figure 3 indicate that equation (19) is valid and verify the theory. In the above results ϵ was determined as a function of agitator frequency, from measured sediment distribution by applying equation (19). Rouse observed a systematic deviation of the value of ϵ obtained for the coarse sand from that obtained from fine sand. The deviation was attributed to a difference in the correlation-factor β of equation (13) for mixing of the fluid and of the sediment.

In 1932 Leighly (15) outlined a method of calculating the exchange coefficient ϵ, for natural streams and discussed its effect in suspending sediment in the body of the flow. In a later paper Leighly (27) calculated the exchange coefficient from some sediment measurements on natural streams by using equation (19). He also calculated the sediment distribution from the exchange coefficient by step integration.

In 1935 Christiansen (28) attempted to check equation (18) by applying it to sediment measurements made by Fortier and Blaney (29) in the Imperial Canal. In general the observations agreed with equation (18) but the results were not entirely conclusive since complete data was not available and it was necessary to estimate such quantities as the slope of the canals, and the settling velocity of the sediment before calculations could be made.

Richardson (30) has made some simultaneous sediment and velocity measurements in the laboratory which led him to conclude that the vertical distribution of sediment is nearly exponential. These experiments were performed in a channel 5 cm wide, 8 cm deep and 150 cm in length, and it is doubtful whether steady conditions could be obtained in such a short

reach. In a later paper (31) this same author reports the results of experiments in a somewhat larger channel (1' x 1' x 6') and concluded that in the boundary region the concentration of suspended sediment is inversely proportional to y and that in the open stream it varies exponentially much as expressed by equation (19). These experiments are subject to the same criticisms as the preceding ones, and it is doubtful if the data can be used to check the theory since the conditions for which relations are developed were probably not attained.

Objective of Experiments

The main objective of the present experiments is to establish the physical law for the distribution of suspended sediment in turbulent open-channel flow and at the same time to verify the theoretical distribution law expressed by equation (25).

In order to accomplish this objective it is clear from equation (25) that in addition to measuring sediment concentration it will be necessary to measure the velocity of flow and the settling rate of the sediment. This will furnish information which can also be used in checking the applicability to open channels of the relations for velocity distribution developed for pipes. Of considerable fundamental importance will be the determination of ϵ, the mixing coefficient, from the measured sediment distribution by using equation (17). Knowledge of this quantity will give further insight into the mechanism of turbulent mixing that will contribute to the complete understanding of the problem.

It is to be emphasized again that once the relations for the dis-

tribution of sediment are established it will still not be possible to predict the total load of the stream. The present experiments will give some data on the total transport. However, complete determination of the relations is obviously not possible within the limited scope of this work. It is also to be pointed out that the present study is only a small part of a comprehensive investigation whose broad objectives are to finally provide laws and relationships that can be used by engineers and other technicians in planning control works where sediment transportation by water is involved.

Apparatus and Procedure

Main flume.

The experiments were performed in a flume 33¼ inches wide by 60 feet long, arranged so the slope and discharge could be varied. The slope was adjusted by means of 4 pairs of screw jacks and the discharge was varied from 1 to about 5.5 cu. ft. per second by changing the speed of the pump in the system through a variable-ratio transmission in the electric motor drive. The sides of the channel were made of 12-inch structural channels lined with 1/8-inch-thick rubber. The bottom was a 5/16-inch steel plate artificially roughened with sand. By making the circulation system closed-circuit with the minimum velocity in the flume, it was possible to recirculate the suspended sediment with the water without danger of depositing material in the piping system.

The flume as first constructed was described in considerable detail by Oaks and Knapp (32) and is shown diagramatically in figure 4.

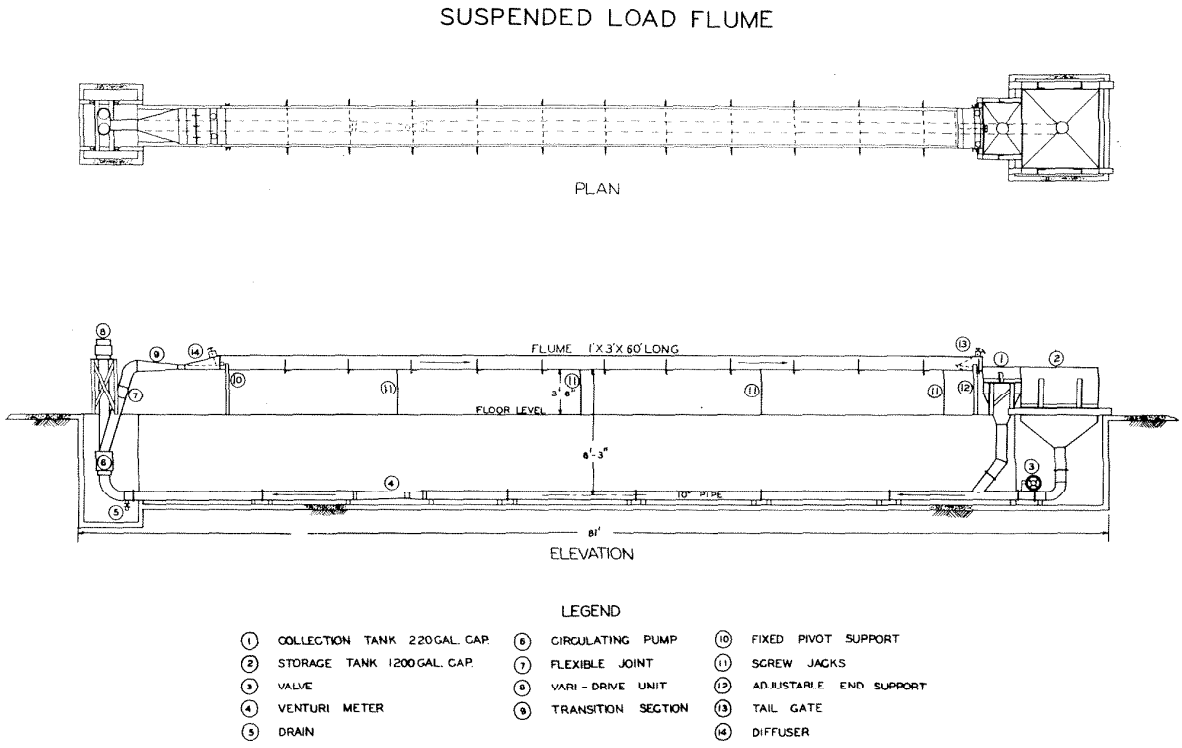

Fig. 4. Flume circuit used for first experiments (series I, Runs 1-13).

Experiments with the above circuit, yielded fair results but indicated that the disturbances due to the pump and inlet were exerting an appreciable effect on flow conditions in the flume. This condition was improved by revising the circuit as shown in figure 5.

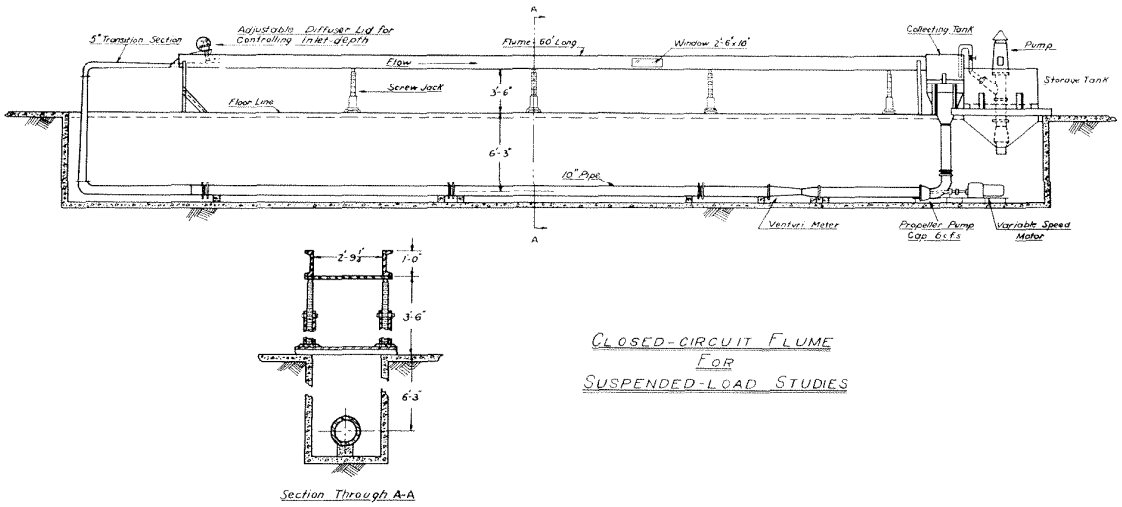

Fig. 5. Revised flume circuit used in final experiments. (series II, runs 14-22).

The pump and venturi meter were placed at the discharge end of the flume, thus providing a run of about 50 feet of 10-inch pipe to "equalize" the flow before entering the transition to the 33½-inch-wide flume section. In order to eliminate the possibility of separation the included angle between the sides of the transition was made 5 degrees.

Particular attention is called to the adjustable horizontal diffuser lid shown in figure 6, which permits the control of the depth at which the water is introduced into the flume section. By this means the upstream depth is made equal to the equilibrium depth in the flume and

uniform conditions are attained in a much shorter reach than would otherwise be possible.

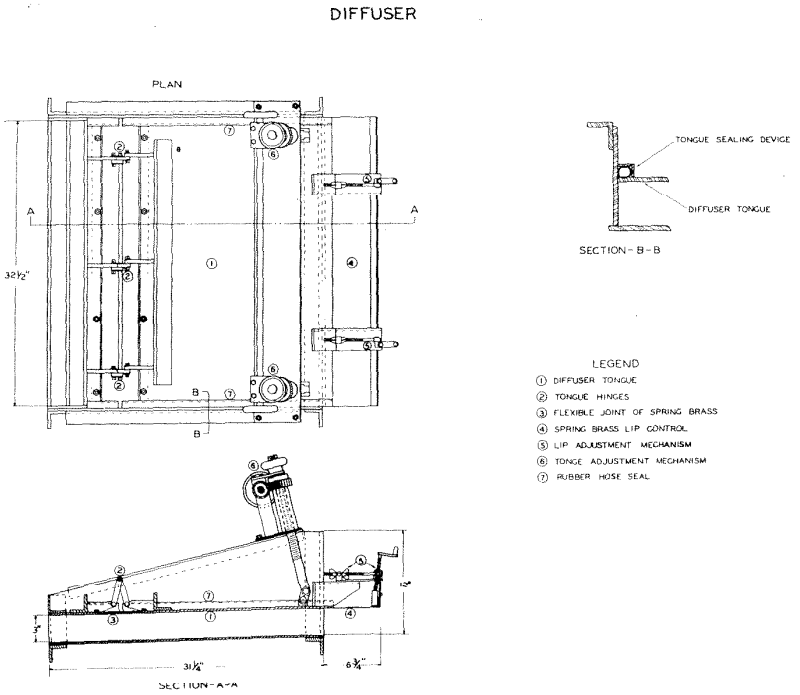

Fig. 6. Diffuser lid at inlet to flume section.

Figure 7 shows the inlet of the flume corresponding to the final circuit shown in figure 5. The adjustable diffuser lid is shown at the left along with the adjusting mechanism, while at the right is seen the down-stream part of the 5-degree transition section. The numbers 1 and 2 on the side of the channel mark the distance in feet from the end of the diffuser lid and are referred to as stations. The flume discharged into a collection tank from which the water and sediment entered a 10-inch pipe and were recirculated.

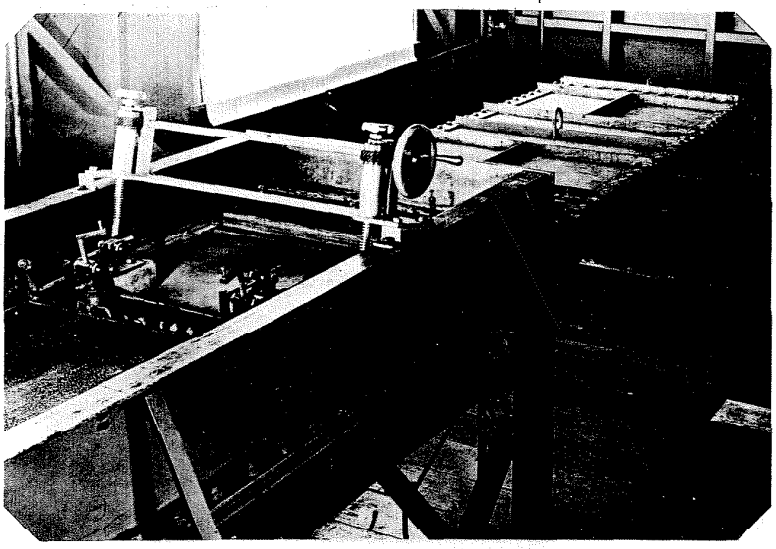

Fig. 7. Inlet to flume showing diffuser lid for controlling inlet depth and downstream end of 5° transition section from 10-inch pipe to flume.

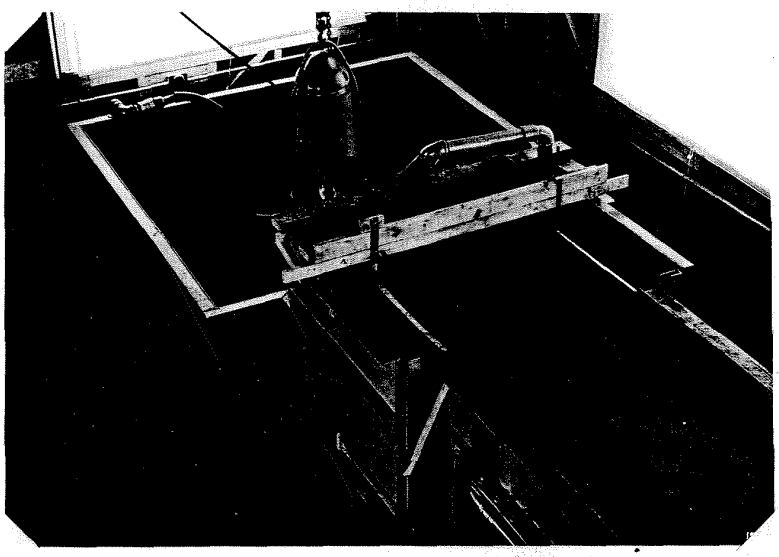

Fig. 8. General view of the discharge end of the flume showing collection and storage tanks.

Figure 8 shows a general view of the discharge end of the flume.

Disturbances of appreciable magnitude in the collector tank tended to

cause air to be entrained and had to be eliminated by properly designed baffles. Horizontal vanes in the baffle in the end of the tank shown in figure 8 helped to turn the flow vertically downward without disturbance. Disturbances that did occur were prevented from reaching the surface by the sheet-metal covering over the vanes. In the background is shown the tank in which the water is stored when the flume is drained. The pump in the center of this tank is used to return the water to the flume.

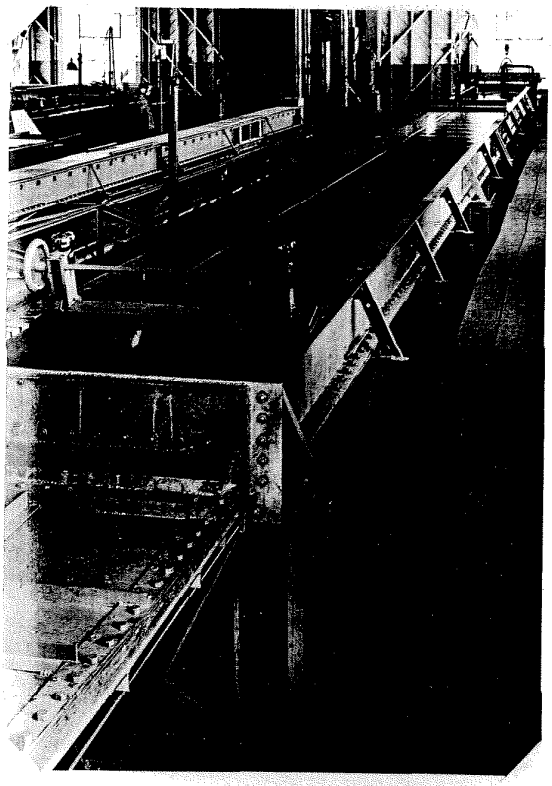

Fig. 9. General view of flume from inlet end.

Figure 9 shows a general view of the flume from the inlet end. The beam spanning the channel at about mid-length carries the instruments used in making measurements.

Adjustment of flow.

Adjusting the flow in the flume to a given depth was readily accomplished by pumping the correct volume of water into the system and varying the discharge until uniform flow was reached. Once the roughness of the channel was obtained from actual measurement of a flow, the discharge for any other depth could be predicted quite closely from the Manning formula. Uniform flow for a given discharge was easily obtained, (once the flow was set with the water manometer on the venturi meter) by adjusting the amount of water in the closed system. No difficulty was ever experienced with the closed system because of pendulation or any other instability. The flow was easily adjusted and remained steady for indefinite lengths of time.

Depth measurements.

Water depths were measured with the point gage shown in figure 10 which can be read to .001 ft. by means of a vernier scale. The procedure in making depth measurements was to first adjust the elevation of the bracket holding the instrument so the scale read zero when the point was resting on the bottom and then to lift the point so it just came in contact with the surface. The scale then showed directly the depth of the water. Considerable judgement had to be exercised in setting the pointer to the surface of the water since waves of some magnitude were always present. The average depth was read from the point gage when the pointer was hitting the water about half of the time. The average depth for the channel was obtained from measurements of at least 10 or 15 points. The mechanism and scale of the point gage were also used

for an instrument holder.

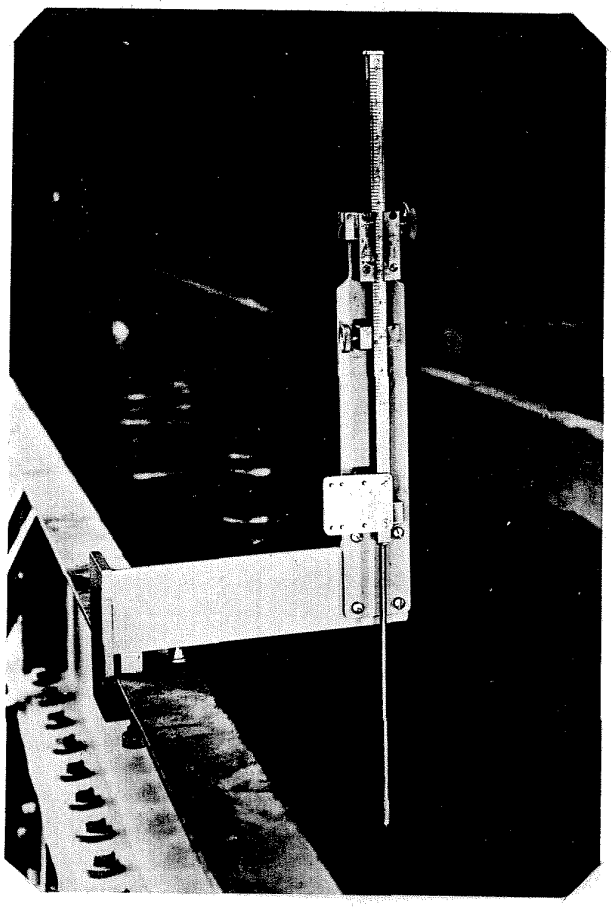

Fig. 10. Point gage for measuring water depth.

Velocity measurements.

Velocities were measured with a 3/16-inch diameter pitot-static tube of the standard Prandtl design. The differential pressure on the tube was read to .001 ft. on a water manometer and converted to velocity by assuming a coefficient of unity for the tube. (That this assumption is justified is shown by Peters (33).)

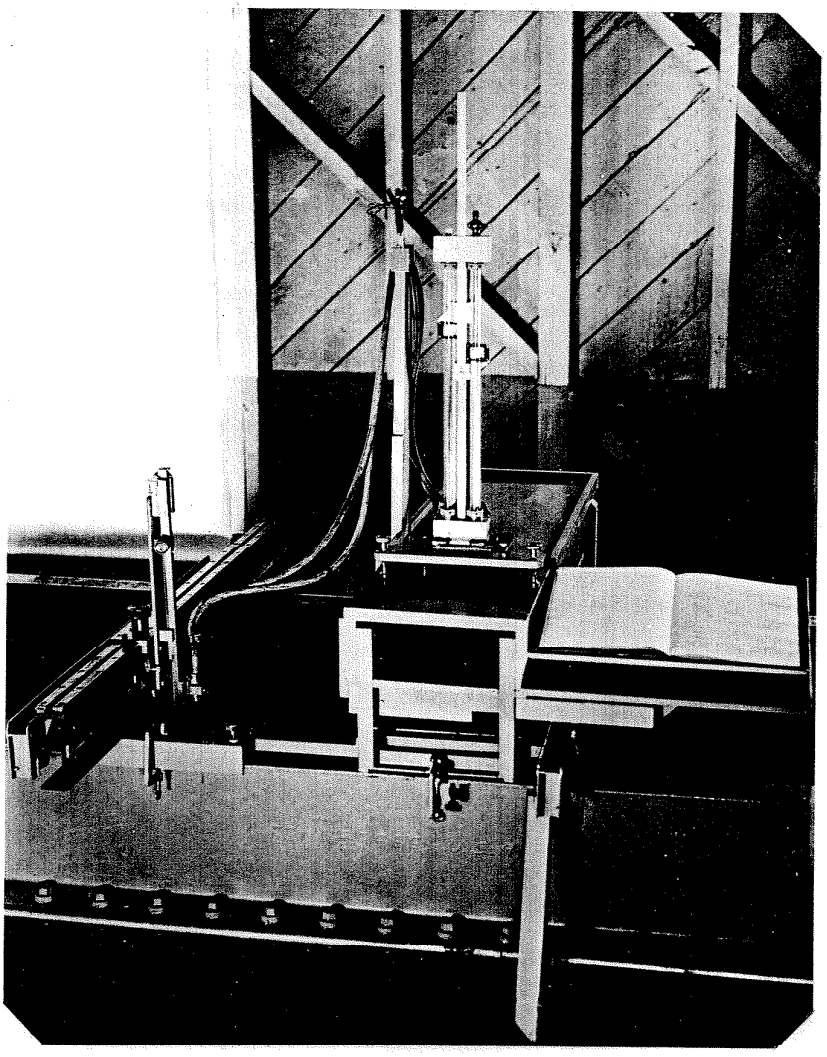

Fig. 11. Pitot-static tube and manometer used in measuring velocities.

Figure 11 shows the set-up used in making velocity measurements. The manometer is shown at the right while at the left the pitot-static tube may be seen mounted in the instrument holder on the cross beam. The entire assembly is arranged so it can be readily moved along the flume on the carriage which is shown in place under the apparatus.

Difficulties from clogging of the pitot tube with sediment in the flow were avoided by frequently flushing it out with tap water passed out through the tube into the stream. Even with this technique there was still some tendency to clog the dynamic port of the tube. However, this was practically eliminated by first introducing water into the manometer, so the differential was greater than the final value and then letting equilibrium be reached. In this manner the flow is always out of the dynamic port and sand is kept from entering the tube.

Frequent additions of clean tap water to the manometer system tended to keep the glass tubes clean, thus reducing errors due to surface tension effects. Before this technique was adopted the menisci of the water columns were often unsymmetrical and poorly formed, but with frequent additions of water this difficulty was eliminated completely.

The manometer was always connected directly to the domestic water line so flushing-out could be done conveniently. Brass cocks at the top of the glass columns and in each of the pressure lines to the pitot-static tube served to control the flow of tap water during the flushing-out operation.

Sediment sampler.

The distribution of sediment was determined from samples siphoned from the flume through a 5/16-inch outside diameter brass-tube pipette shaped much like a pitot tube. The tip of the sampler, which is shown in figure 12, was flattened so its inside dimensions were 0.490 inches by 0.139 inches. The average velocity at which the sediment-laden fluid entered the flat tip section was made equal to the stream velocity at

the sampling point, by adjusting the head on the siphon.

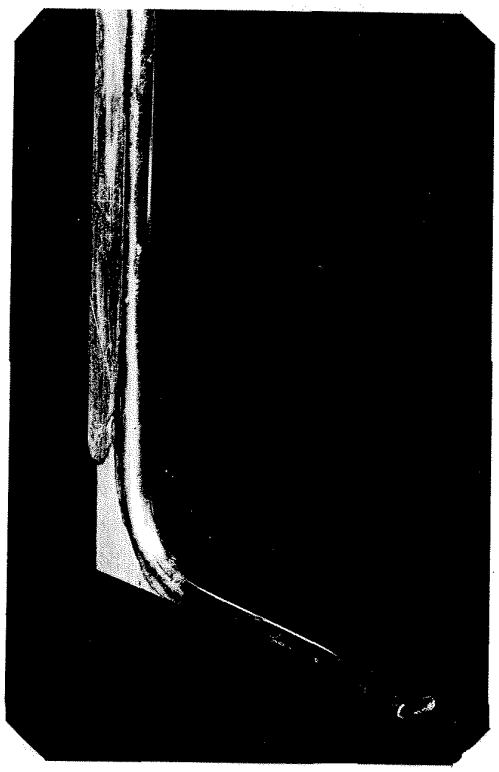

Fig. 12. Flat tip of 5/16-inch brass-tube sampler used in obtaining suspended load samples.

Figure 13 shows the set-up used in sampling. The elevator in the center, which carries the end of the siphon and the liter sample bottle, permits convenient adjustment of the head on the siphon which can be read directly from the scale on the right post of the elevator. The end of the siphon was mounted on a pair of sliding shafts so the flow could be quickly shifted from the sample bottle to the waste and vice-versa. Attention is called to the station numbers on the side of the flume. Samples are being taken at station 40.

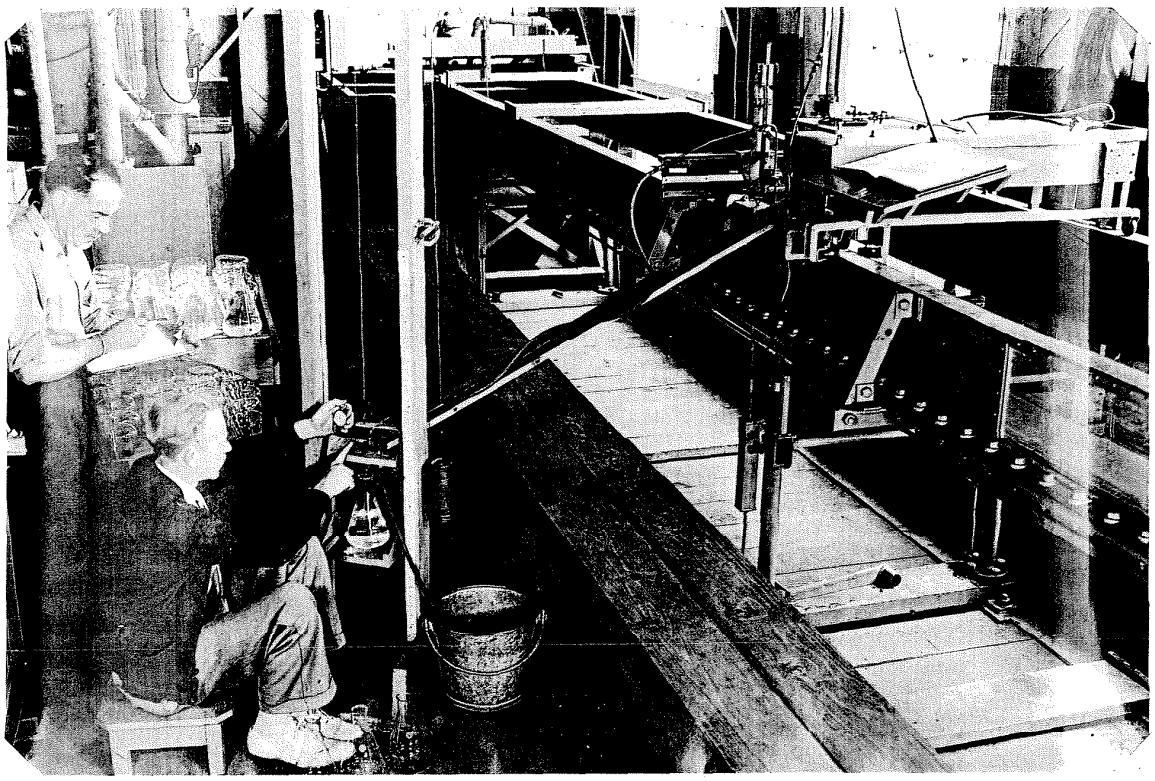

Fig. 13. Set-up for taking suspended-load samples.

The time to remove a 1-liter sample was calculated for each point from the measured stream velocity and the area of the flat tip sampler (.064 sq. in.), the head on the siphon required for the rate of flow determined by trial, and three liter samples taken. The time for each sample was measured with a stop watch and recorded. The sediment was removed from the sample by filtering and was dried and weighed. The average weight of the three samples was taken as the concentration at the point. Weights of over 1 gram were determined to 1 centigram while the smaller quantities were determined to 1 milligram.

Water removed from the flume in sampling was replaced in order

to keep the depth uniform. It was found that removing or adding as little as 3 gallons of water made a measurable difference in the tail-water depth.

The effect of the rate of sampling on the amount of sediment removed with the sample was studied experimentally. A series of liter samples were removed from a point at rates (velocities of the fluid at entrance to the flat tip sampler) corresponding to 1.00, 0.86 and 0.75 times the local stream velocity. The sampling point was 0.5 feet from the center of the flume, 44 feet from the inlet, i.e., at station 44, and 0.1 feet from the bottom. The local velocity was 3.19 ft/sec., the flume was set to a slope of .0025 and the water was flowing at an equilibrium depth of 0.495 feet. The suspended load had a mean settling rate in still water of 0.058 ft/sec.

The results of this experiment, presented in Table I, show that as the sampling rate decreases, the amount of sediment collected per given volume of fluid increases. When the sampling velocity is lower than the local stream velocity, the fluid stream lines curve away from the sampler tip. Due to their greater inertia the sediment particles follow paths of less curvature than the fluid with the result that sediment is transferred to the fluid entering the sampler and the apparent concentration is increased. When the sampling velocity is greater than the stream velocity the curvature is toward the sampler, and, therefore, a tendency to decrease the amount of sediment collected would be expected.

The values of $\frac{c}{C}$ in Table I give some idea of the fluctuation in concentration at a point in the flow. While the deviation of individual sample weights from the mean was as high as 10 percent, it is interesting

TABLE I

Experimental determination of the effect of relative sampling velocity on the amount of sediment collected. U = local stream velocity (3.19 ft/sec). U_s = velocity of fluid at entrance to flat-tip sampler.

$\frac{U_s}{U}$	$\frac{C}{\bar{C}}$	$\bar{C}$ gr. per liter	$\frac{\bar{C}}{\bar{C}_1}$
1.00	0.99 1.04 0.99 0.95 0.97 1.06	1.03 $(\bar{C}_1)$	1.00
0.86	0.98 0.94 1.08 0.90 1.00 0.99 1.05 0.91 1.10	1.08	1.05
0.75	1.13 0.99 0.95 0.99 1.00 0.97	1.12	1.09

C = sediment collected in grams per liter.
$\bar{C}$ = average value of C for given rate of sampling.

to note that the deviation of the average of three consecutive sample weights from the mean does not exceed 3 percent. It is also interesting to note that the length of a filament of fluid having a volume of one

liter and an area equal to that of the sampler tip is well in excess of the length of the flume, i.e., 60 feet.

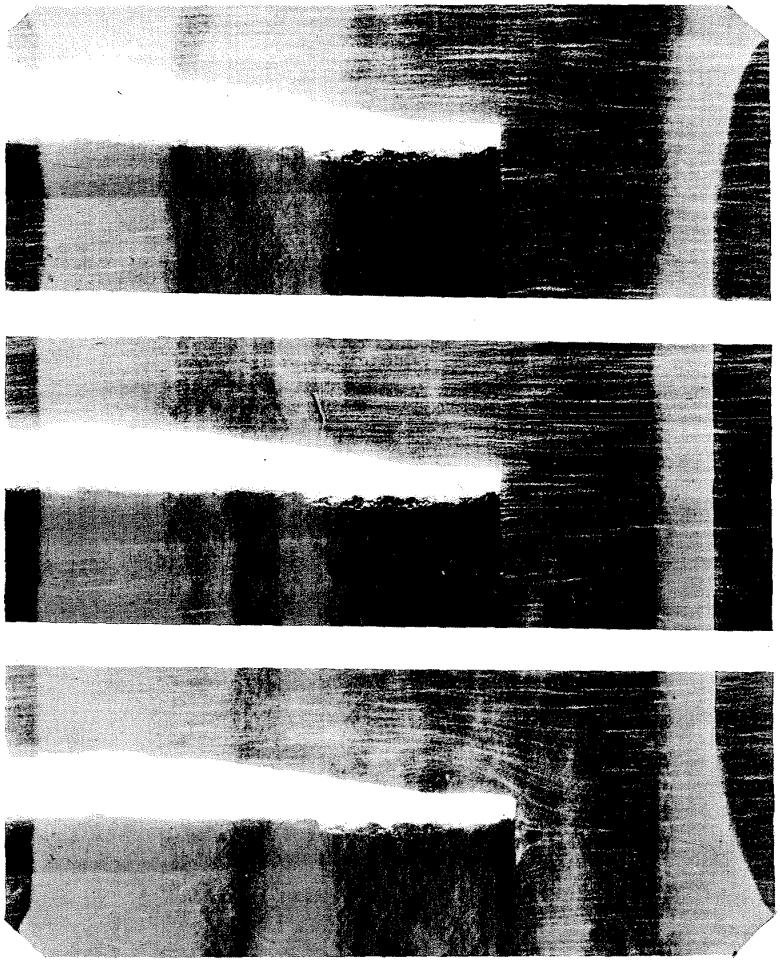

Fig. 14. Photographs of sampler operating in stream at different relative sampling rates, U_s/U.

Figure 14 shows three photographs of the flat-tip sampler operat-

ing at ratios of sampling velocity to stream velocity $\frac{U_s}{U}$ of (a) 1.0, (b) 0.7, and (c) 0.0. The center photograph (fig. 14b) shows very clearly the curvature away from the sampler, while the lower photograph indicates that even for no flow in the sampler some sediment enters the tube.

Sediments used as suspended load.

Sediments used as suspended load were prepared by grading a silica sand in a wind-tunnel classifier constructed for this purpose. This device, which is described by Otto and Rouse (34), is arranged so that sand is introduced into the upper part of a horizontal wind stream and is collected in pans along the bottom of the stream. For any wind velocity the horizontal distance traveled by the particles is determined by their settling velocity so material collected at a point on the bottom is well sorted as to settling rate or hydraulic diameter.

Figure 15 shows a logarithmic-probability plot of sieve analyses of the three sands used as suspended load. The table within the figure shows the size parameters of the sediments. The quantity d_m is the geometric mean sieve diameter and is read directly from the plot. For a normal distribution, i.e., straight line on plot, the geometric mean and median diameter are equal. The quantity σ_g is known as the geometric standard deviation of the sieve diameters. It is the ratio of the geometric mean size, d_m, to the size that passes 16.2 percent of the material which in turn is also equal to the ratio of the size passing 83.8 percent of material to d_m. The method of calculating these parameters was shown by Otto (35).

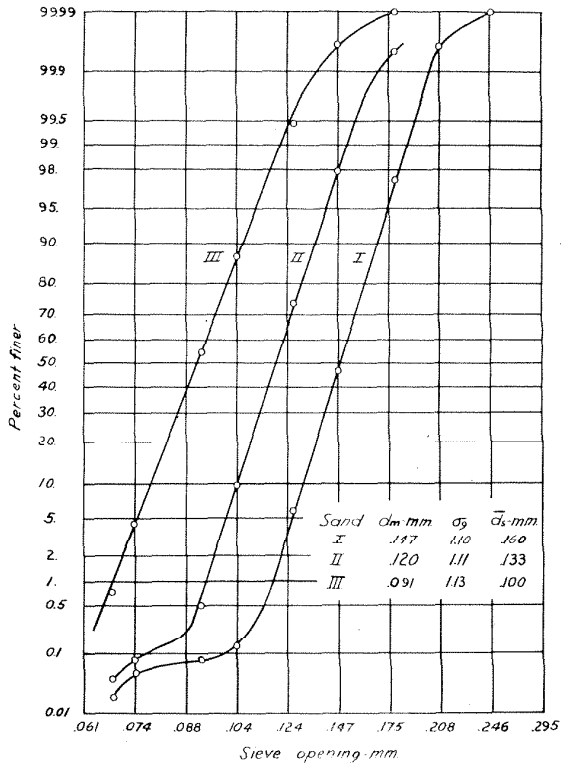

Fig. 15. Logarithmic probability plot of sands used as suspended load.

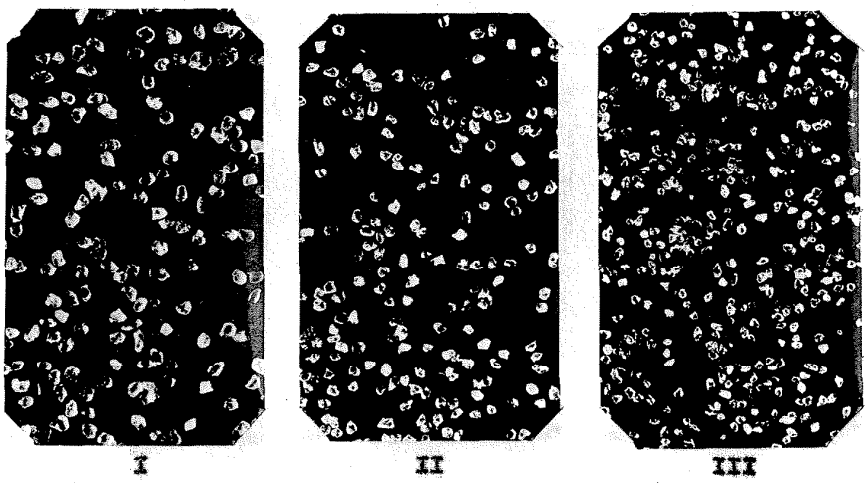

I II III

Fig. 16. Photomicrographs of sands used as suspended load. (magnification 10 diameters).

Figure 16 shows photomicrographs of the three sediments whose mechanical analyses are plotted in figure 15. The sand grains are quite well rounded and uniform in shape.

The quantity $\overline{d_s}$, in figure 15 is the mean sedimentation diameter where the sedimentation diameter of a particle is defined as the diameter of the sphere of the same density having the same settling velocity as the particle. The geometric mean settling velocity w, in water was determined from observed settling times for individual particles of a representative sample of the sediment. The mean sedimentation diameter is then the diameter of the quartz sphere having the settling velocity w , in water.

Calculation of the sedimentation diameter was based on the resistance coefficients for spheres as outlined by Rouse (36). This operation was considerably simplified by using curves of settling velocity versus diameter of sphere for various values of the temperature (fig. 2a). The mean sedimentation diameter was also determined from sieve analyses by taking a weighted mean of the sedimentation diameters of the material held in each sieve. This latter diameter was determined from actual settling velocity measurements of samples taken from the sieve separates. The procedure in making the sedimentation-diameter determinations is described in detail in Appendix I.

The average sediment concentration for the entire flow was determined from samples siphoned from the collection tank through a 3/4-inch pipe and rubber hose. The entrance of the siphon was directed vertically upward so the downward flow in the tank could enter without changing di-

rection. During sampling the pipe was moved around so fluid was obtained from all parts of the cross section. In general the velocity in the tube was greater than the velocity of flow at the sampling point and according to the preceding discussion one would expect the sample to show less concentration than actually existed.

Bottom roughness.

As mentioned previously, the sides of the flume were lined with rubber while the bottom was roughened with sand. The two bottom roughnesses used in the experiments were formed by the sands whose sieve analyses are plotted in figure 17.

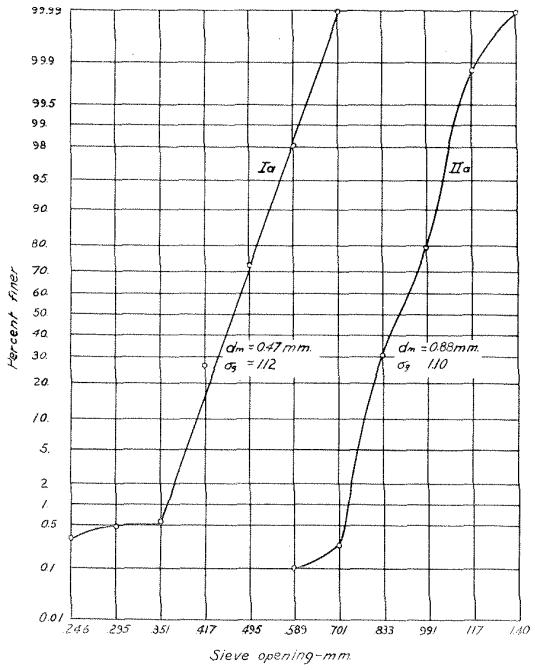

Fig. 17. Logarithmic probability plot of sieve analyses of sands used to roughon bottom of flume.

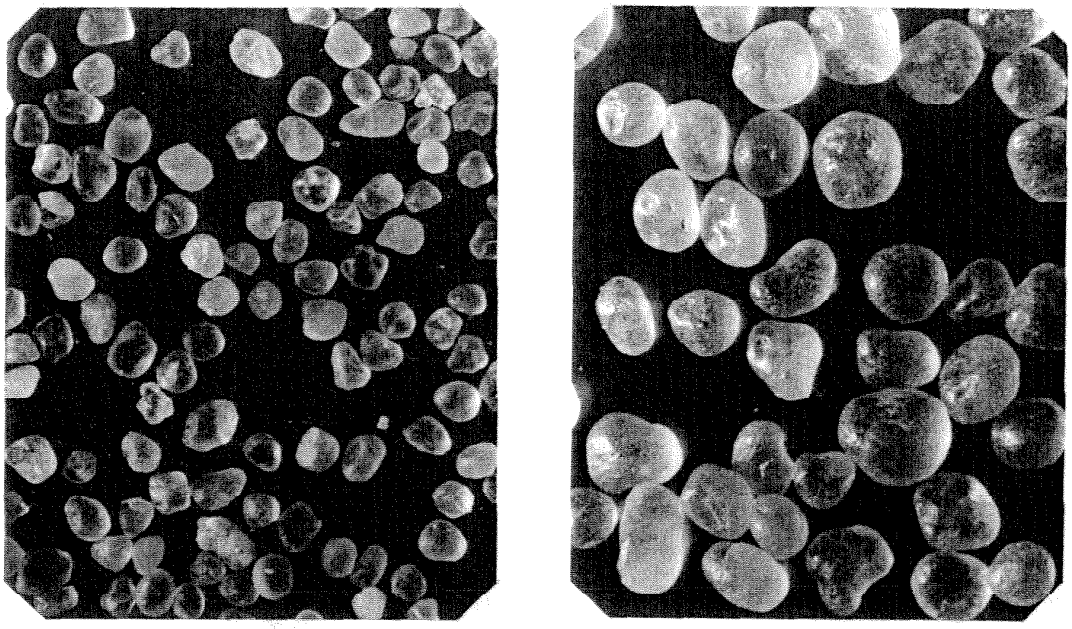

I (a) II (a)

Fig. 18. Photomicrographs of sands used to roughen bottom of flume. (magnification 10 diameters).

Figure 18 shows photomicrographs of the same sands. Sand I (a) was separated from the same sand that the suspended-load materials I, II and III were obtained from. The source material is used locally as a foundary sand and is called "Nevada white sand". Material II (a) is also silica and is quarried in Wisconsin and sold locally under the trade name "gold jacket". As the trade name indicates, the material is coated with a gold-colored substance that gives it a distinctive appearance. The above sands were graded in the wind-tunnel classifier described previously.

The sand was stuck to the flume bed with a water-resistant black bitumastic paint. The metal surface was first painted and the sand immediately applied in sufficient quantity to cover the surface at least one

layer deep. The excess material was swept off after the paint was dry, leaving a uniform sand bed one grain in thickness.

RESULTS

General outline of experiments

The experiments on this study may be divided into two series. In the first series, which was carried out in the flume circuit shown in figure 4, the slope of the flume (s = .0025) was kept constant and only one bottom roughness (sand Ia) and one suspended load (sand I) were used. Only the rate at which water was discharged and the amount of sediment in the system were varied. As mentioned under "Apparatus and Procedure" this circuit (fig. 4) gave a disturbed entrance condition and was not considered completely satisfactory. The disturbances were due to the pump, which was near the inlet to the flume and to separation of the flow in the transition from the pipe to the flume. The latter was remedied, at least in part, by baffles which, of course, introduced considerable resistance and, therefore, turbulence. A good index of the performance of the system is given by the head loss or the head developed by the pump which amounted to about 5 feet for a discharge of 5 cubic feet per second.

The second series of experiments was made in the revised circuit shown in figure 5. No separation occurred in the transition section and the velocity distribution was quite uniform and symmetrical. Only about 3 feet of head was required to circulate 5 cubic feet of water per second in the revised system. In this series, complete measurements were made with one bottom roughness, (sand IIa), three sizes of suspended load and two depths at each of two slopes thus covering a fairly wide range of conditions.

Velocity distribution

Equation (29) for the distribution of sediment over a vertical section of a stream was derived for a flow with a large width-depth ratio, i. e., two dimensional conditions and for the case of logarithmic velocity distribution. Before the relation can be applied to the present experiments it is necessary to show that the assumed conditions obtain. Figure 19 shows the velocity distribution across the flume for the first series of experiments, i. e., series I (Runs 1-13) while some typical velocity distribution curves for series II (runs 14-22) are shown in figure 21. Comparison of figure 21, (a to d) with figure 19, (d to f) shows at once the improvement in the flow effected in series II by changing the system from that shown in figure 4 to the one in figure 5. These velocity distributions also show that the influence of the walls of the channel does not extend to the center of the flume and that the assumption of two dimensional conditions near the center of the flume is justified. The only way that the resistance of the walls can be transferred to the center of the channel is by turbulent shear or momentum transfer which can exist only if there is a horizontal velocity gradient. The fact that this gradient is zero or very small permits the conclusion that near the center of the flume the influence of the walls is negligible.

Figure 19, (d to f) and figure 21, (a to d) give the velocity distribution at various stations, i. e., distances from inlet, along the flume and show the gradual stabilization of the velocity front. Here again may be noted the improved flow conditions in series II (fig. 21).

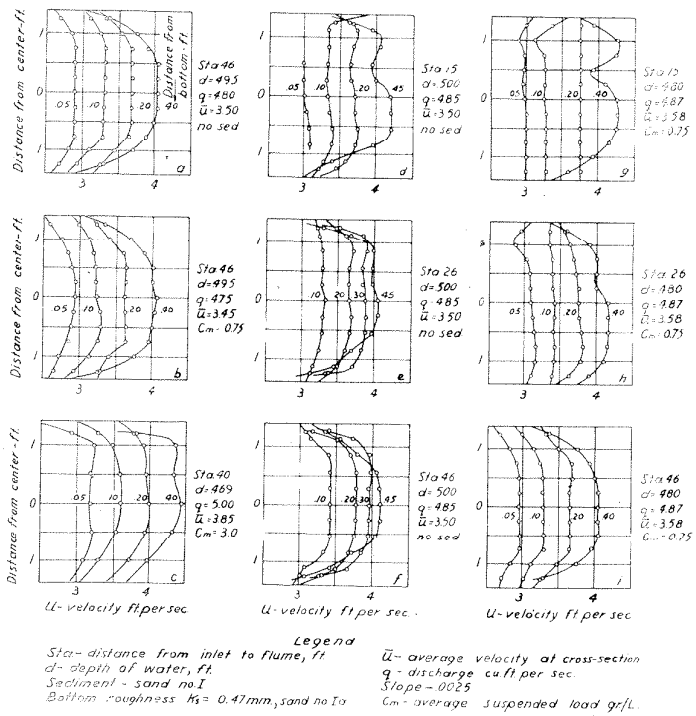

Fig. 19. Velocity distribution over cross section of flume for series I. (Bottom roughness 0.47 mm sand, slope = .0025. See fig. 4 for circulation system)

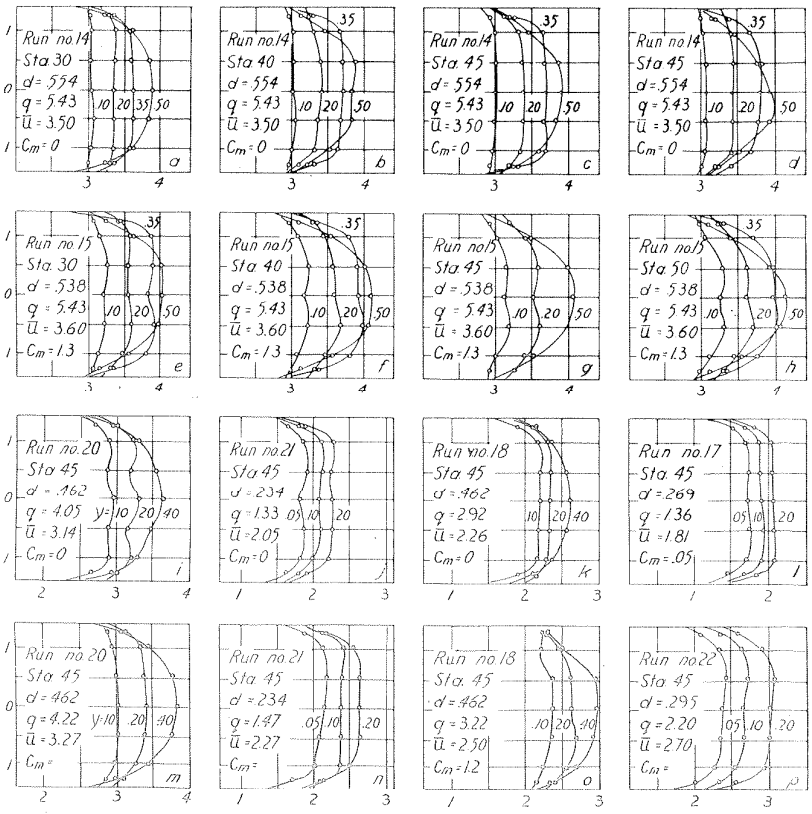

Fig. 21. Velocity distribution over cross section of flume for series II (Bottom roughness 0.88 mm sand. (See fig. 5 for circulation system)

Despite the higher discharge, the velocity assumes a stable configuration, quite near the inlet, that obtains over the remaining length of the flume. The distortion of the velocity at depth 0.5 feet at station 50 (fig. 21-d) is due to backwater from the discharge end which is at station 57. Figures 19 and 21 also show the effect of the sediment on the flow. This point will be discussed in a later section.

Figures 20 and 23 show dimensionless semi-logarithmic plots of velocity profiles for series I and II, respectively. The relative distance from the bottom, $\frac{y}{d}$, is plotted on the logarithmic ordinate scale against the dimensionless velocity $\sqrt{gds}$ on the abscissa scale. The quantity $\sqrt{gds}$ is the so-called friction velocity commonly written $\sqrt{\frac{\tau_o}{\rho}}$. The abscissa scale is shifted for each curve as may be seen in the figure, the abscissa value 15 being indicated for each curve. The curves in figure 20 are arranged into four groups according to the average sediment content of the flow, while those in figure 23 are grouped according to size of the sediment being transported.

In all cases the velocity distribution fits the logarithmic law very well. There is a systematic deviation from the law as the bottom is approached which may be attributed to the effect of viscosity. In exerting its influence the viscosity tends to suppress the turbulence which has the effect of lessening the exchange coefficient, ϵ, in the equation,

$$\tau = \rho \epsilon \frac{dU}{dy} \qquad (5)$$

In order to develop the shear, the decrease in the mixing coefficient

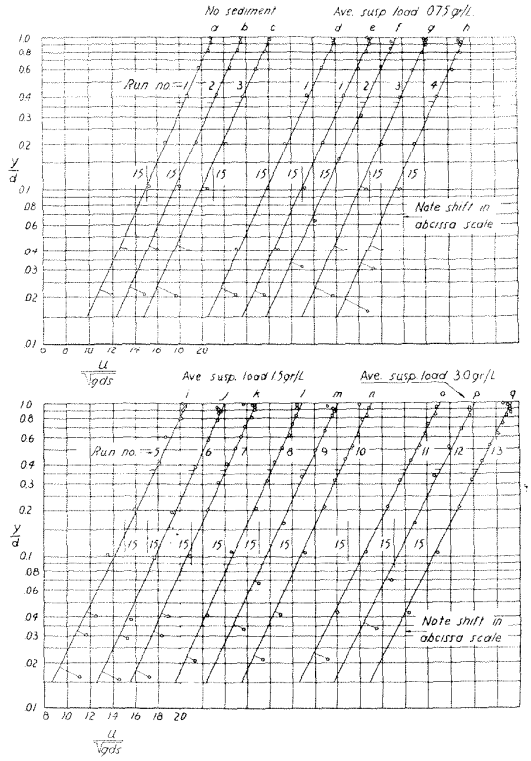

Curve	k	Curve	k
a	.375	j	.364
b	.368	k	.365
c	.372	l	.368
d	.366	m	.355
e	.365	n	.360
f	.362	o	.332
g	.371	p	.333
h	.369	q	.334
i	.351		

Fig. 20. Plot of velocity profiles on center of flume for runs 1 to 13. (series I)

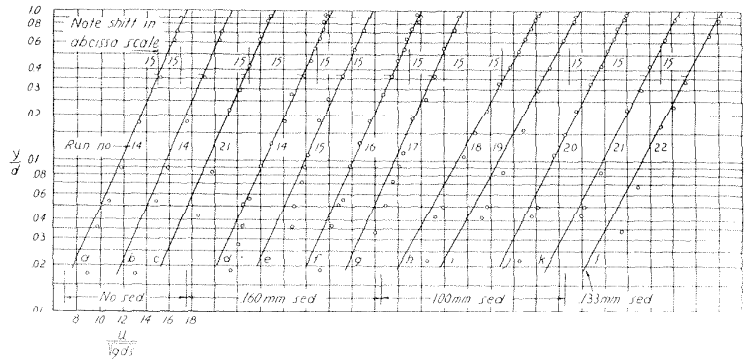

Curve	k
a	.397
b	.397
c	.392
d	.386
e	.384
f	.385
g	.386
h	.314
i	.320
j	.349
k	.332
l	.341

Fig. 23. Plot of velocity profiles on center of flume for runs 14 to 22 (series II)

is compensated for by an increase in the gradient which results in the increased velocity near the bottom. It is to be noted that the deviation from the law occurs in the lower 10 percent of the depth and that it is therefore not of major importance as far as the distribution of the sediment in the main body of the flow is concerned. An apparent deviation from the law is also to be noted at the free surface. However, due to surface waves and the disturbance of the pitot tube itself it is felt that these measurements are not too reliable and that conclusions based on them must be drawn with reservation.

The velocity curves of figures 20 and 23 are of the form,

$$\frac{U}{\sqrt{gds}} = \frac{U\ max}{\sqrt{gds}} + \frac{2.3}{k} \log \frac{y}{d} \qquad (31)$$

where k is a universal constant. The quantity 2.3/k is the slope of the semilogarithmic plot of the velocity profiles which should be constant if k does not vary. A close inspection of figures 20 and 23 will show that the slopes of the curves do vary, as the size and concentration of sediment are varied. The values of k for the individual curves are shown in tables to the right of the figures and in table II, columns 6 and 7. In general, k decreases as the concentration is increased or as the size of sediment in suspension is decreased.

Figures 22 and 24 show the velocity profiles for series I and II, respectively, plotted according to the von Kármán velocity defect law, equation (26). In figure 22, the data of figure 20 have been combined according to the sediment content of the flow and shows clearly the variation of k. In figure 24, the data of figure 23 have been

TABLE II

Complete summary of Experiments

Col.No.		1	2	3	4	5		6	7	8	9	10	11	12	13	14	15	16
Line No.		Run No.	Slope s	Depth d	$\sqrt{gds}$	Location Sta.	Location Dist. from Center	K	Ave. K.	$\bar{K}_1$	Reference Fig. No.	Temp. Deg.C.	w f.p.s.	$\frac{w}{2\sqrt{gds}}$	Z_1	Reference Fig. No.	Ca gr/L	$\bar{C}$ gr/L
1		1	.0025	.181	.197	46	0.0	.375		3.62	20-a		No	0.0	0.0		0.0	0.0
2		2	"	.196	.200	44	0.0	.368	0.372	3.60	20-b		sed.	0.0	0.0		0.0	0.0
3		3	"	.181	.197	44	0.0	.372		3.45	20-c			0.0	0.0		0.0	0.0
4							0.0	.366		3.60	20-d	23.6	.0522	.723				
5		1	"	.181	.197	46	0.0	.365	0.370	3.63	20-e	21.8	.0485	.672	.67	25-a	2.60	0.72
6							0.5L	.374		3.63		22.6	.0492	.672	.67	25-b	2.80	
7							0.5R	.374		3.63		21.2	.0478	.663	.67	25-c	2.62	
8		2	"	.314	.159	46	0.0	.362	0.362	2.80	20-f	19.0	.0450	.775	.67	25-d	3.33	0.35
9		3	"	.196	.200	44	0.0	.371	0.371	3.58	20-g	23.3	.0590	.805	.80	25-e	3.80	0.85
10							0.5L	.371		3.58		24.4	.0602	.822	.82	25-f	4.00	
11		4	"	.192	.199	44	0.0	.366	0.369	3.63		20.8	.0564	.771	.77	25-h	3.18	0.79
12							0.5L	.369		3.64	20-h	23.3	.0590	.815	.97	25-g	3.20	
13							0.0	.351		3.57	20-i	23.1	.0590	.818	.83	25-i	4.30	
14		5	"	.196	.200	44	0.5L	.351	0.351	3.48		23.8	.0596	.826	.86	25-j	4.65	1.79
15							1.0L	.359		3.31		24.4	.0603	.835	.86	25-k	4.70	
16		6	"	.518	.204	44	0.0	.373	0.369	3.97	20-j	23.8	.0596	.810	.81	25-l	9.25	1.78
17							0.5L	.364		3.94		26.3	.0626	.850	.83	25-m	7.35	
18							0.0	.365		3.62	20-k	25.1	.0610	.845	.85	25-n	6.40	
19		7	"	.198	.200	44	0.5L	.371	0.368	3.63		26.5	.0626	.868	.91	25-o	7.00	1.61
20							1.0L	.418		3.43		27.4	.0636	.850	.91	25-p	7.30	
21		8	"	.183	.197	40	0.0	.363	.365	3.79	20-l	26.6	.0626	.880	.87	25-q	8.35	1.34
22							0.5L	.369		3.72		27.8	.0636	.895	.97	25-r	9.63	
23		9	"	.303	.156	40	0.0	.355	.355	3.05	20-m	24.7	.0511	.960	.96	25-s	7.80	1.141
24							0.5L	.355		3.00		24.7	.0511	.960	.97	25-t	7.45	
25							0.0	.360		3.82	20-n	26.3	.0626	.870				
26		10	"	.178	.196	40	0.5L	.360	.360	3.76		26.8	.0626	.870			Not	Not
27							1.0L	.360		3.64		27.7	.0636	.899			meas.	meas.
28							1.0R	.372		3.50		28.5	.0643	.908				
29							0.0	.332		3.97	20-o	27.0	.0650	.970	.97	25-v	19.6	
30		11	"	.174	.195	40	0.5L	.332	.332	3.85		28.2	.0643	.990	1.01	25-w	18.6	3.36
31							1.0L	.332		3.73		25.8	.0620	.955	1.10	25-u	22.9	
32							0.0	.333		2.97	20-p	24.8	.0568	1.10	1.04	25-x	12.9	
33		12	"	.299	.155	40	0.5L	.333	.333	2.97		25.7	.0578	1.12	1.02	25-z	11.9	2.56
34							1.0L	.333		2.85		26.2	.0585	1.13	1.06	25-y	11.7	
35		13	"	.478	.196	46	0.0	.334	.334	4.81	20-q	24.9	.0580	0.886	0.85	25-aa	11.0	3.19
36		14	"	.554	.211	40	0.0	.397		3.58	23-a							
37		14	"	.554	.211	45	0.0	.397		3.39	23-b							
38		20		.162	.193	45	0.0	.389	.394	3.21			0.0	0.0	0.0		0.0	0.0
39		21	"	.234	.137	45	0.0	.392		1.99	23-e							
40		14	"	.538	.208	45	0.0		.386	3.46	23-d	24.0	.0590	.729	.89	27-m	9.09	1.33
41		15	"	.274	.118	45	0.0	.384	.384	2.54	23-e	21.0	.0577	1.02	1.02	27-n	5.85	.55
42		16	.00125	.557	.117	45	0.0	.385	.385	2.70	23-f	21.4	.0577	1.02	1.05	27-o	3.02	.59
43												20.0	.0571	1.13	1.02	27-s	0.535	
44												20.0	.0571	1.13	1.08	27-p	0.036	
45		17	"	.269	.104	45	0.0	.386	.386	1.77	23-g	19.3	.0567	1.12	1.15	27-r	0.995	.018
46										1.82		19.6	.0567	1.12	1.17	27-q	0.116	
47	Series II							.314		2.57		19.0	.0269	.630	.53	27-d	4.79	
48		18	"	.162	.136	45	0.0	.314	.317	2.48	23-h	20.0	.0275	.644	.54	27-e	4.89	1.18
49								.321		2.55		22.0	.0285	.667	.58	27-c	3.54	
50								.317		2.45		21.6	.0285	.667	.54	27-f	4.25	
51						45	0.0	.334		1.87		23.2	.0292	.897	.63	27-g	.949	
52						40	0.0	.334		1.82		21.1	.0282	.866	.64	27-h	.999	
53		19	"	.236	.0975	40	0.0	.334	.330	1.78		19.2	.0272	.835	.69	27-i	1.20	.1 69
54						45	0.0	.334		1.78		20.3	.0275	.845	.68	27-j	1.14	
55						45	0.0	.320		1.82	23-i	20.5	.0278	.854	.64	27-k	1.29	
56		20	.0025	.162	.193	46	0.0		.349	3.24	23-j	22.0	.0285	.1488	.54	27-m	1.27	
57		21	"	.234	.136	46	0.0	.332	.332	2.28	23-k	19.7	.0275	.609	.42	27-b	3.42	
58		22	"	.295	.154	45	0.0		.341	2.60	23-l	17.8	.0207	.775	.46	27-l	6.75	

$\frac{z_1}{}$ = Value of exponent (eq. 29) for best fit of experimental data.

$\frac{}{C}$ = Measured average concentration over cross section. Bottom roughness; series I, 0.47 mm sand; series II, 0.88 mm sand (see fig. 17)

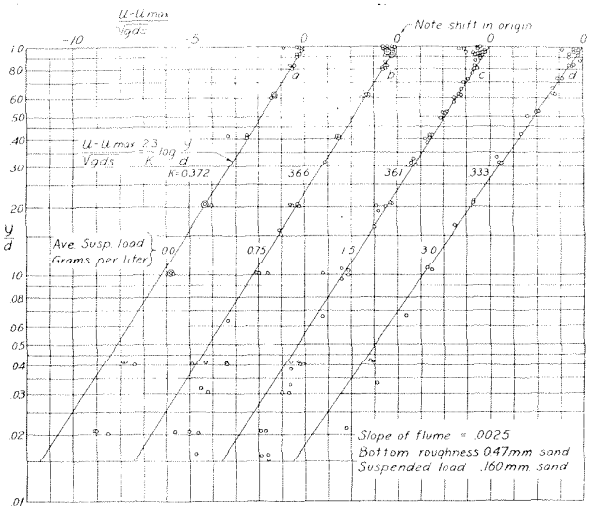

Fig. 22. Velocity profiles for series I for several concentrations of suspended load

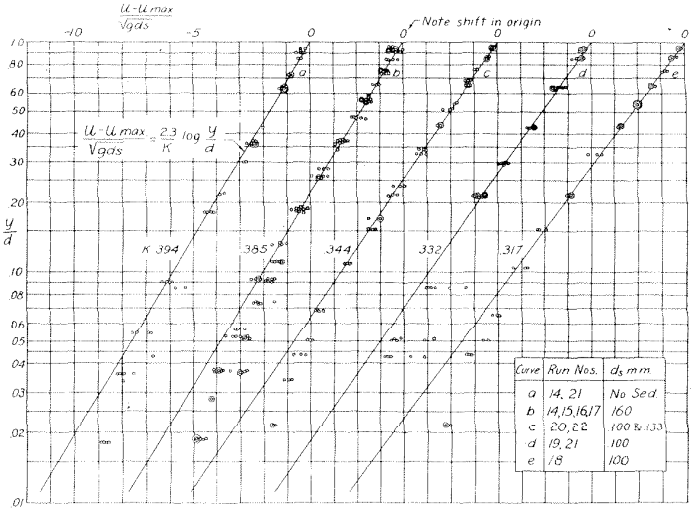

Fig. 24. Velocity profiles for series II for three sizes of suspended load

grouped according to the values of k. The curves show that k is decreased by the presence of the sediment but the relation between size of sediment and the universal constant, k, is not clear. Figures 22 and 24 do show, however, that the logarithmic velocity law is valid and justify its use in developing equation (29) for suspended load distribution.

Distribution of Suspended load

Equation (29) plotted logarithmically is a straight line with a slope,

$$z = \frac{\text{Log}\frac{C}{Ca}}{\text{Log } H} \qquad (32)$$

which may be read directly from the graph. Figures 25 and 27 show the sediment distribution data for series I and II, respectively, plotted in the above manner, i. e., log C/Ca against log H. The origin of the abcissa scale (log H), which occurs at C/Ca = 1, is shifted for each curve.

The value of z may also be calculated from the expression,

$$z = \frac{w}{k\sqrt{\frac{\tau_o}{\rho}}} = \frac{w}{k\sqrt{gds}} \qquad (33)$$

where w is the settling velocity of the sediment, k is the von Kármán universal constant and $\sqrt{\frac{\tau_o}{\rho}}$ is the friction velocity. In order to distinguish between the value obtained by equation (33) and that obtained by fitting the experimental data in figures 25 and 27, the latter value is denoted by z_1. Obviously, if the theory is correct the two values will agree.

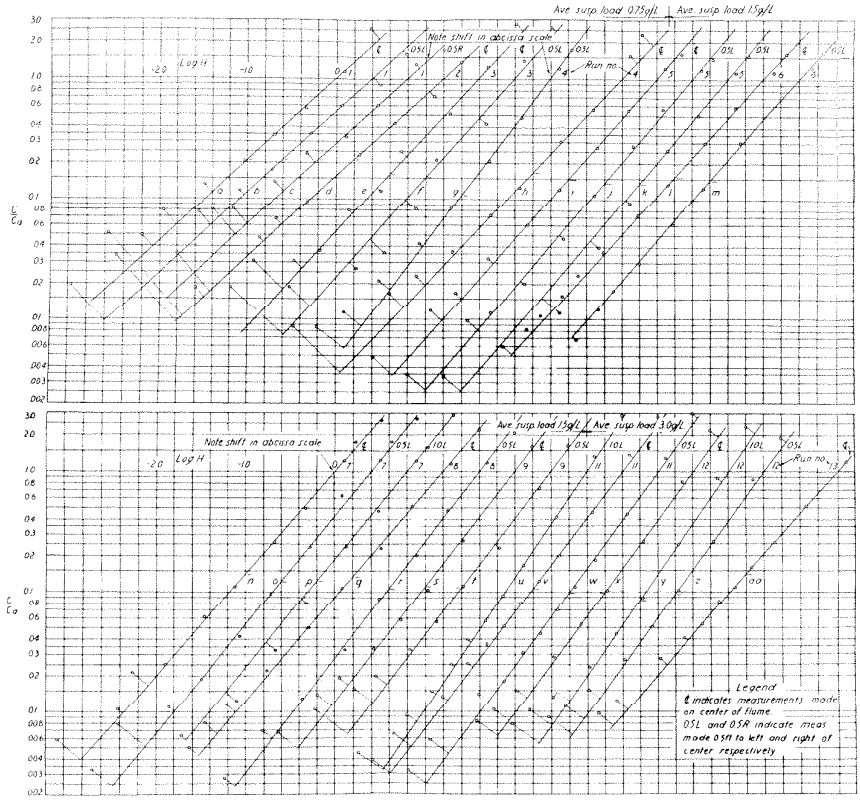

Fig. 25. Plot of measured sediment concentration against the distribution function, H, for series I.

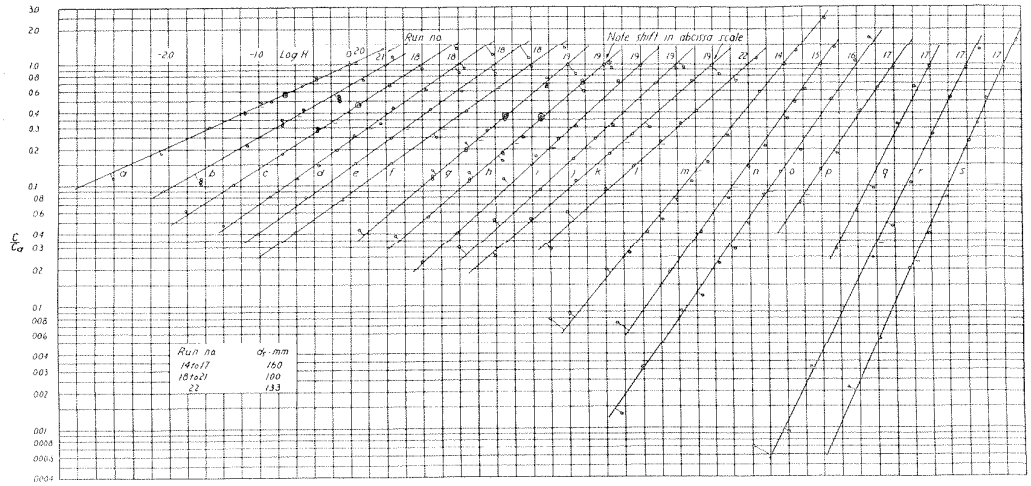

Fig. 27. Plot of measured sediment concentration against the distribution function, H, for series II.

The intersection of each curve with the line log H = 1.0 is indicated by a short horizontal dash. The vertical distance from the origin (C/Ca = 1) to the dash, measured in cycles on the logarithmic scale is the value of z_1. The values of both z and z_1 are listed in table II (cols. 12 and 13). The two values agree quite well for runs 1 to 17 which were all made with the coarsest suspended load (sand I). For all of the runs with finer sand the value of z is from about 20 to 40 percent greater than z_1.

From inspection of figures 25 and 27, it is at once apparent that the results of series II are in much closer agreement with the distribution law (equation (29)) than those of series I. The disagreement occurs in the upper levels of the flow, i.e., for small values of H, where more sediment is found than would be expected from the law. Comparison of the results of the two series must be made only for those runs made under comparable conditions with the same size sediment. Runs 14 to 17 of series II were made with the same sediment as the runs of series I and may therefore be compared. These runs (14-17) also show more sediment in the upper levels than given by equation 29 but the difference is slight. The rather large departures from the distribution law in series I are no doubt due to entrance disturbances in the flow which, as pointed out previously, were appreciable compared with those occurring in the revised circulation system (fig. 5) used in series II.

The disagreement between the theoretical and measured concentrations shown in figures 25 and 27 are, in final analysis, quite small

and the curves show conclusively that at least the form of the distribution function is correct. This conclusion is confirmed by figures 26 and 28 which show plots of z_1 log H against log C/Ca for series I and II. Here again the disagreement in the upper levels between measurement and the distribution function is noticeable as is also the better agreement of the results of series II.

Figures 29 and 30 show the sediment distribution, both measured and calculated, (equation 29) as a function of the relative depth measured upward from the reference level a = .05d. The measurements are indicated by circles while the theoretical distribution is shown as a solid line. The agreement for series II (fig. 30) as previously seen is quite good over the entire depth, whereas series I (fig. 29) shows the departure in the higher levels noted before.

It is well to note that in calculating the sediment distribution the experimental values, z_1, of the exponents were used. Table II, Cols. 12 and 13 shows agreement between z and z_1 for only one sediment so it is not possible to say that the distribution law (equation 29) gives the correct values of the relative concentration, C/Ca. What can be said is that the distribution function is of the correct form. The significance of the lack of agreement in some cases between z and z_1 will be discussed below.

Coefficient of turbulent mixing

The turbulent mixing coefficient is given by equation (20),

$$\epsilon = BV^1\ell = \frac{\tau}{\rho \frac{dU}{dy}} \qquad (20)$$

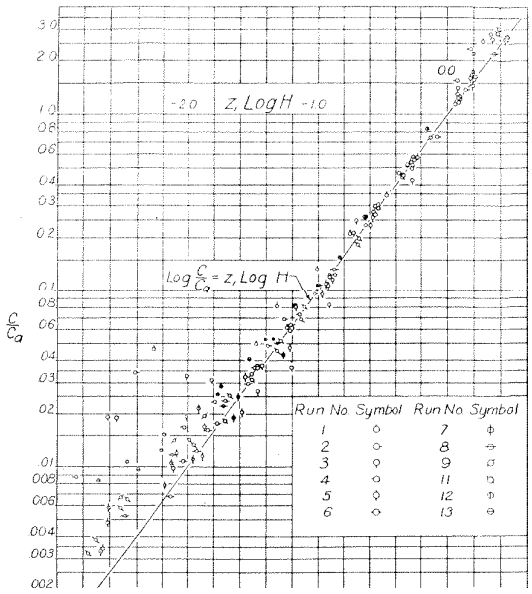

Fig. 26. Plot of measured against calculated sediment concentrations, for series I.

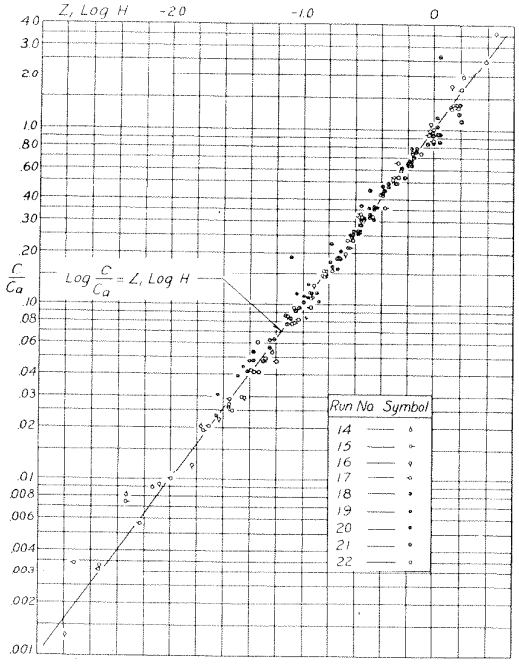

Fig. 28. Plot of measured against calculated sediment concentrations, for series II.

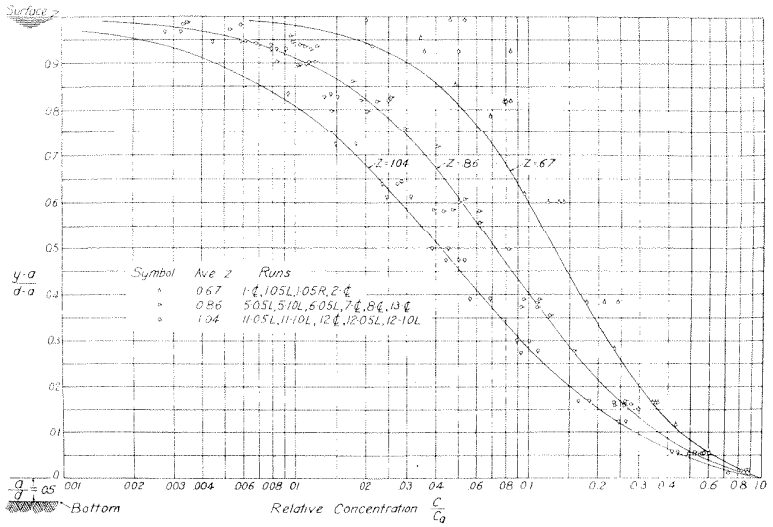

Fig. 29. Plot of measured and calculated sediment concentrations as a function of relative depth for series I

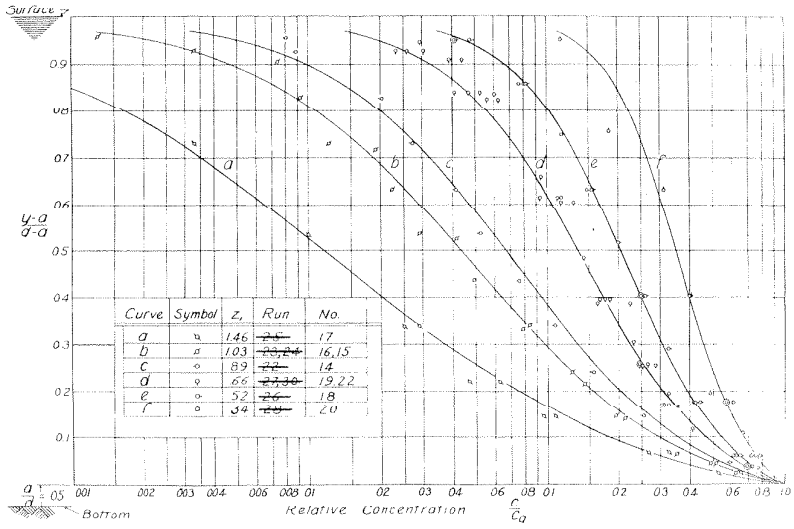

Fig. 30. Plot of measured and calculated sediment concentrations as a function of relative depth for series II

Introducing equations (23) and (27) into (20) gives,

$$\epsilon = BV'l = k\sqrt{\frac{\tau_o}{\rho}}\left(1 - \frac{y}{d}\right)y \qquad (34)$$

This expression assumes logarithmic velocity distribution and linear distribution of shear and gives the coefficient ϵ, for momentum transfer. In deriving equation (29) the assumption was made that the mixing coefficient for momentum would also apply to sediment transfer. The measured sediment distribution now makes it possible to calculate the mixing coefficient for the sediment by applying equation (17) which gives,

$$\epsilon = \frac{wC}{\frac{dC}{dy}} \qquad (35)$$

The mixing coefficients may be reduced to a dimensionless form by dividing by the depth times the friction velocity as follows:

$$\frac{\epsilon}{d\sqrt{gdS}} = k\left(1 - \frac{y}{d}\right)\frac{y}{d} \qquad (36)$$

and,

$$\frac{\epsilon}{d\sqrt{gdS}} = \frac{w}{\sqrt{gdS}} \times \frac{C}{d\frac{dC}{dy}} \qquad (37)$$

Figure 31 shows both the mixing coefficient for momentum (eq. 36) and for sediment (eq. 37) for four identical flow conditions. The a and b curves of the figure are for series I with average suspended loads of 1.34 and 3.36 grams per liter (see table II, col. 16), respectively, and in general are typical of this series. Curves c and d are typical of results obtained in series II, the former being for

the coarsest sediment (sand I) and the latter for the finest sediment (sand III).

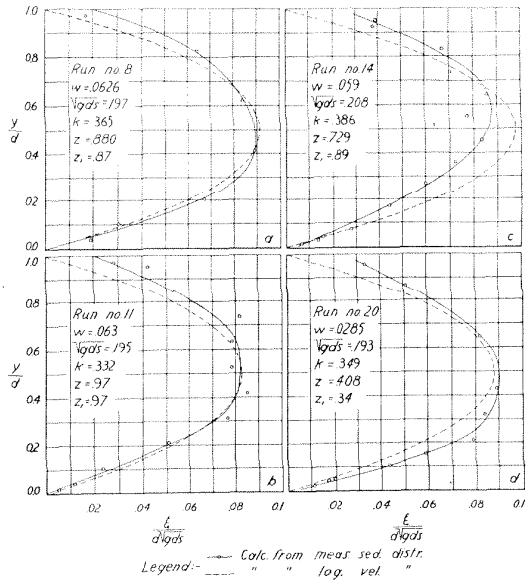

Fig. 31. Mixing Coefficients ϵ, for momentum transfer and sediment transfer

The agreement between the two mixing coefficients for series I (fig. 31a and b) is quite good. For the coarse sediment in series II, the sediment coefficient is smaller than the momentum coefficient, while the opposite is true for the fine sediment. Equation (18) shows immediately that small values of ϵ give small values of the concentration, C. It is also apparent from equation (29) and figure 2 that increasing ϵ, and therefore C, will tend to make the concentration more uniform, i.e., decrease z. These effects may be noted in figure 31 c and d. In the former case, the ϵ value for sediment mixing is less than assumed, i.e., less than the coefficient for momentum transfer,

and the measured value of z (0.89) is greater than the predicted value (.729), while in the latter case the reverse is true, i.e., $z_1 < z$. In estimating the effect of ϵ on the sediment distribution it is well to note that ϵ appears in an integral and that departures from the assumed values exert a cumulative effect.

DISCUSSION OF RESULTS

Effect of suspended load on the velocity distribution

The von Kármán universal constant k, (eq. 26 and 31) depends only on the mechanism of turbulent mixing and a change in k means that the mixing mechanism has in some way been altered. From equations (5) and (27),

$$\epsilon = ky\frac{\tau}{\rho\sqrt{\frac{\tau_o}{\rho}}} \qquad (38)$$

or the mixing coefficient is directly proportional to k. A decrease in k decreases the mixing coefficient and if the shear (depth and slope) is kept constant the velocity gradient will have to increase to compensate for the reduced ϵ. This will result in an increase in the velocity of flow. Thus it is seen that k is also a factor in establishing the velocity distribution.

The values of k obtained for various sediments and flow conditions are shown in table II, columns 6 and 7. The effect upon k of increasing the sediment load is shown by series I, i.e., runs 1 to 13. As the load was increased (see table II, col. 16) the k values decreased. Series II, i.e., runs 14 to 22, shows that the coarse sediment (.160 mm) although reducing k somewhat has less effect than the finer sediment. In general, for the fine sediment, k appears to decrease as the friction velocity $\sqrt{gds}$ decreases. However, there does not appear to be any simple relationship between the various factors. From the above results one would expect k to be a function of w, the

settling velocity of the sediment, the average sediment load and the friction velocity $\sqrt{gds}$. Further analysis and investigation will be required to completely explain the effect of sediment on the flow.

The sediment might be thought of as tending to suppress the vertical components of the turbulence, thus making the transfer of momentum less effective. (The late Mr. Henry M. Eakin advanced this idea to the writer in 1936 during a discussion of the suspended load problem.)

Attention is called to the lack of agreement between the values of k obtained in series I and II for similar flows. For instance, the average k for clear water for series I was 0.372 while for series II it was 0.394. No straightforward explanation of these results can be offered. However, the difference is most likely due to the difference in the inlet conditions for the two series of experiments. The k value obtained for series II which was run with very good flow conditions checks very well with that obtained for pipes and it is quite reasonable to assume that the results of this series are more reliable than those of series I.

The effect of suspended load on the resistance to flow

As remarked in the preceding discussion, a reduction in k results in an increased velocity which will also give a reduction in the resistance coefficient of the channel. The Chezy formula for flow in conduits is,

$$\overline{U} = c\sqrt{RS} \qquad (39)$$

where $\overline{U}$ is the mean velocity in the cross section, c is the Chezy coefficient, R is the hydraulic mean depth, i.e., area of cross section devided by wetted perimeter, and S is the slope or pressure gradient. c for open channels is given by the Manning formula,

$$c = \frac{1.486}{n} R^{\frac{1}{6}} \tag{40}$$

where n is a roughness coefficient. The Chezy coefficient can also be expressed in terms of f, the resistance coefficient.

$$c = \sqrt{\frac{8g}{f}} \tag{41}$$

Equations (39) (40) and (41) can be solved for n and f with the following result:

$$n = \frac{1.486}{\overline{U}} R^{\frac{2}{3}} S^{\frac{1}{2}} \tag{42}$$

$$f = \frac{8g}{\overline{U}^2} RS \tag{43}$$

Several values of n and f for flows with and without sediment are shown in table III.

The effect of the suspended load in reducing the resistance is clearly seen. The reduction in both n and f appears to be the same for the two sediments but is greater for the low flows than for the high flows.

Buckley (38) observed from measurements on the Nile that suspended load decreased the roughness coefficient of the river channel. An average sediment load of 1.7 grams per liter gave n = .025 while for

clear water n was found to be .042, which is a much larger effect than expected from the present experiments. Buckley attributed the reduction in resistance to the damping effect of the sediment on the turbulence in the vicinity of the bed of the stream.

TABLE III

Resistance Coefficients with and without Suspended Load

Run No.	d	$\overline{U}$ f.p.s.	n	$\frac{n_w}{n_s}$	f	$\frac{f_w}{f_s}$	Sed. dia. mm	$\overline{C}$ gr/L
14	.554	3.56	.0113	1.05	.0201	1.07	None	0.0
14	.538	3.65	.0108		.0187		.160	1.33
18	.462	2.28	.0114	1.11	.0215	1.22	None	0.0
18	.462	2.52	.0103		.0176		.100	1.18
20	.461	3.16	.0117	1.04	.0224	1.09	None	0.0
20	.462	3.30	.0112		.0205		.100	1.12
21	.234	2.05	.0124	1.10	.0306	1.22	None	0.0
21	.234	2.27	.0113		.0250		.100	1.07

n_w and f_w = Coefficient with clear water
n_s and n_s = Coefficient with suspended load

Distribution of suspended load.

All the measurements of suspended load distribution followed very closely the form of the sediment distribution law, equation (29), but agreement between the calculated and measured value of the exponent z, occurred only for the coarsest suspended load (d_s = .160 mm). For the finer sediments the value of the exponent that fit the data, i.e., calculated value, was about 20 percent less than the value

indicated by the theory. As noted previously, a decrease in z causes the sediment to distribute itself more uniformly over the depth or in other words it behaves as a finer sediment.

The mixing coefficient ϵ, is given by

$$\epsilon = \beta v' \ell \tag{13}$$

and has the same form for both momentum and sediment mixing but not necessarily the same value (von Kármán (11)). For a fine sediment the mixing coefficient for momentum was smaller than the corresponding coefficient for sediment transfer. It can readily be seen that increasing ϵ will tend to produce a more uniform sediment distribution which results in z_1 being smaller than z.

The difference between the coefficient for sediment and momentum transfer can be accounted for, at least in part, by the action of the random turbulence in supporting sediment. For momentum transfer a correlation is required between the velocity fluctuations. However, for sediment transfer the correlation is not necessary and random velocity fluctuations also carry sediment. The experiments show that as the sediment gets finer the sediment coefficient exceeds the momentum coefficient. This would indicate that the coefficient for sediment transfer is a function of w, the settling velocity of the sediment. In view of the above remarks, it appears that the good agreement between z_1 and z for the coarse sediment is merely a coincidence and that if still coarser sediment had been used the disagreement between z and z_1 would have been of the opposite sign, i.e., z would be smaller than z_1.

Although it is possible to calculate the numerical values of

ϵ for the sediment and momentum transfer it is not possible to assign values to each of the factors β, ν' and l. It seems reasonable to expect that ν' for the sediment transfer should not differ appreciably from the corresponding value for momentum transfer and that most of the difference between the sediment and momentum coefficients should be accounted for by β and l.

The tendency for the sediment content near the surface of the flow to exceed that indicated by the distribution equation (29) can be explained by the action of the random turbulence. Although the mixing coefficient for momentum goes to zero at the surface the random fluctuations carry sediment right up to the very surface, thus giving the mixing coefficient for sediment a finite value at the surface. This can be noted in figure 31.

Attention is called to the wide disagreement between the measured and calculated values of z in the first two sediment profiles of run 17 (table I, cols. 12-13, lines 43-44). Considerable difficulty was experienced in this run in getting the sediment to distribute itself uniformly over the cross section. Since the flow was very low and the sand coarse, considerable material was moving along the bottom and any lack of uniformity in the distribution was easily noticed. The first measurement (line 43, table II; and curve s, fig. 27) was made over a point where considerable sediment was in motion in a narrow band on the bottom. The abnormally large value of z could be accounted for by the occurrence of a transverse transfer of sediment in the horizontal direction away from the measuring point, brought

about by the existence of a concentration gradient across the flow. In the same way it is possible to account for the low value of z obtained in the second measurement of run 17 (line 44, table II). In this case the measurements were taken over a point where very little sediment was in motion on the bed but a few inches to one side of the section considerable sand was being carried. The transverse transfer of sediment into the measuring section decreases the vertical concentration gradient and therefore the value of z that will fit the data. It is surprising that even under such conditions the distribution should follow the law.

Instability and secondary flow due to suspended load

The effect of the suspended load was first noticed in measuring the velocity distribution over cross sections of the flume. Distributions that were quite uniform with clear water became quite distorted by the addition of very small amounts of sand. This effect may be noted in figure 19 a, b and c which show the velocity distribution for clear water, and for average sediment concentrations of 0.75 and 3.0 grams per liter, respectively. To give an idea how small the concentrations actually were, it might be well to remark that the first concentration (Cm = 0.75) was obtained by adding only 12.5 pounds of sand to the entire system. The effect of this small concentration on the flow may also be seen by comparing the center column of figure 19 with the right column. The effect is small for this small concentration but it is noticeable. Incidentally, before leaving figure 19, attention is called to the uniform spacing of the velocity lines, es-

pecially in (a). This shows at once that the velocity distribution is logarithmic since the distances from the boundary (y) are spaced geometrically.

The disturbing effect of the sediment is also shown in figure 21. The top line of curves, i.e., figures 21 a-d, for clear water may be compared with the second line which shows the velocities with corresponding conditions with sediment in the flow. Figures 21-i and m show a case where the sediment apparently has a stabilizing effect. For this particular case, the conditions were apparently just right to establish good flow at this particular station. The fact that the velocity with clear water was distorted serves to illustrate again that the sediment has considerable influence on the flow.

In observing the flow it was noticed that the sediment appeared to be transported in clouds or ribbons parallel to the flow. At low flows when appreciable material was moving along the bottom, these ribbons appeared as bands of sand on the bottom. When proper flow conditions had been attained, these ribbons were symmetrical and quite stable over the entire range of flow. Attempts to break them up artificially were only partially successful. Figure 32 is a photograph of these bands of sediment taken after run 15, looking upstream. The photograph was taken after the flow had been stopped and the water slowly drained off. Material in suspension settled to the bottom, thus showing how it was distributed in the fluid. Three main streaks are shown in the center portion of the flume while two less pronounced streaks occur at the walls. This pattern, which was quite symmetrical,

Fig. 32. Sediment distribution on floor of flume as deposited by the flow of run No. 15

occurred over the entire length of the flume. Measurement of suspended load at a distance of .02 feet from the bottom showed that the distribution was quite uniform over the center half of the flume, then suddenly dropped to about 15 percent of the center concentration as the clear areas (fig. 32) were approached and finally increased to about 50 percent of the center value near the walls. The concentration for the center 6 inches was about 5 percent less than that over the concentrated streaks at the side. (The flume is 33¾ inches wide by 12 inches deep).

The cause of these longitudinal bands of sediment is not known, although it is felt that they are due to secondary circulation and disturbances due to the presence of suspended load. Even the slightest departure from a uniform sediment distribution will cause horizontal density gradients that can set up secondary flows. The sediment distribution described above shows a concentration gradient and one could then expect a circulation with an upward flow at the points of low concentration and a downward flow where the load was high. Since there are three points of low concentration, three pairs of circulations might be expected. No direct observations were made to attempt to check this hypothesis and it is doubtful if this could be done without considerable work. However, this is a possible explanation of the action of the sediment in distorting the flow. Further investigation will show whether or not this idea is valid.

If circulation could be caused by sediment in a carefully controlled laboratory channel, it was felt that the possibility of its

occurrence in natural streams with irregularities and disturbances was even greater. With this idea in mind measurements of suspended load in rivers were examined. Figure 33 a and b shows measurements at a cross section of the River Po reported by Giandotti (30).

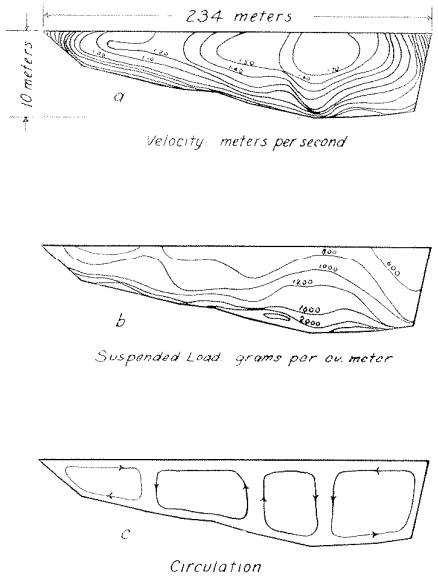

Fig. 33. Velocity and sediment measurements on the River Po (Giandotti) and expected circulation due to sediment

Note the high concentration of suspended load at about the $\frac{1}{4}$ points of the section. The circulation expected from this distribution is shown in figure 33c. The writer is not able to state whether or not this distribution is typical of rivers. However, in this case there is certainly evidence that a circulation can be caused by the sediment. The circulation that would be induced is the same as that advanced as an explanation for the depression of the maximum velocity in natural streams. Although this circulation explained the velocity distribution,

no satisfactory explanation was ever found for the circulation itself. The distribution of sediment furnishes a fairly reasonable and probable explanation of this mysterious phenomenon.

Sediment transporting capacity.

Equation (29) may be integrated over the depth to give the average value of the relative concentration over a profile, as follows:

$$\frac{\overline{C}}{C_a} = \frac{1}{d-\delta}\int_{\delta}^{d} K^z dy \qquad (44)$$

where δ is some small value of y. If then, the value of C_a is known, the average concentration can be calculated from equation 44 and the load of the stream determined. Figure 34 shows a plot of this function for $a = \delta = .05d$ upon which have been plotted the results of the second series of experiments.

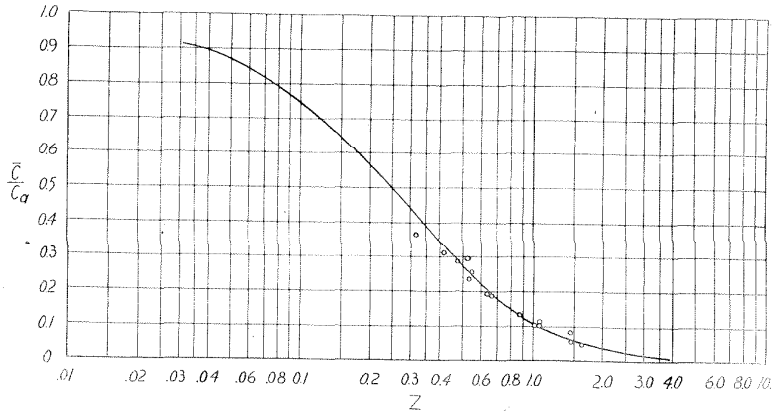

Fig. 34. Plot of average relative concentration against z.

In discussions of sediment transportation reference is

frequently made to the "capacity" of a stream to carry sediment. The term is loosely used but in general it is taken to mean the amount of a given sediment that a flow is capable of carrying, i.e., hold in suspension. If the material is relatively coarse, i.e., large z, little material is suspended and one would expect the stream to have a small capacity. For fine materials, i.e., small z, a much larger capacity is to be expected and in some cases, such as in mud flows, the capacity seems to be without limit.

Rather small amounts of sand were used in the present experiments and it is doubtful if enough material was ever available to completely load the flow except for the very low velocities, i.e., large z. In series I of the experiments three amounts ($12\frac{1}{2}$, 25 and 50 lbs.) of sand were used as suspended load. Columns 15 and 16 of table II show that C_a and the average sediment concentration varied about as the total sand in the system, and that no capacity was ever reached. (Column 16 of Table II was determined from samples taken from the end tank and represents an average for the entire flow.)

In the second series of experiments, the value of $\overline{C}$ increases as z decreases. However, if more sediment were added, it is possible that $\overline{C}$ would still increase without appreciably altering z as occurred in series I. It is apparent that further study of this problem is necessary before it can be understood.

Calculation of the average velocity for logarithmic velocity distribution.

Assume a velocity distribution following the von Kármán

universal velocity defect law,

$$\frac{U - U_{max}}{\sqrt{\frac{\tau_o}{\rho}}} = \frac{1}{k} \log_e \frac{y}{d} \qquad (26)$$

The average velocity defect is given by,

$$\frac{\overline{U} - U_{max}}{\sqrt{\frac{\tau_o}{\rho}}} = \frac{1}{kd} \int_{\delta}^{d} \log_e \frac{y}{d} \, dy \qquad (45)$$

where δ is a small value of y and $\overline{U}$ is the average velocity. Solution of equation 45 gives,

$$\frac{\overline{U} - U_{max}}{\sqrt{\frac{\tau_o}{\rho}}} = -\frac{1}{k} \qquad (46)$$

Eliminating the velocities between equations 46 and 26 there follows,

$$\log_e \frac{y_a}{d} = -1$$

and

$$y_a = \frac{d}{e} = .368d \qquad (47)$$

where y_a is the distance from the bottom to the point where the average velocity occurs. Thus it is seen that the average velocity is always located at a constant relative depth as long as the velocity distribution is of the logarithmic-form. This distance is independent of the roughness or the value of k.

In the present experiments the average velocities were determined by graphical integration of the velocity profile and by the above rule (eq. 47). The two results agreed within 1 or 2 percent.

In figures 20 and 23 the value $y/d = .368$ is indicated at each curve by a short dash and the average velocity can be read directly from the curves. The velocities in column 8 of table II were determined by the above rule.

Experience in stream gaging has shown that for all practical purposes the average velocity in a vertical occurs at six-tenths of the depth below the surface, i.e., $\frac{y}{d} = 0.4$, or that it is the average of the velocities at the 0.2 and 0.8 depths. The agreement between the rule developed above and the rule developed by experience is quite good. Also for logarithmic velocity distribution the average of the velocities at the 0.2 and 0.8 depths ($y/d = 0.8$ and 0.2) is exactly equal to the velocity at the 0.6 depth. This is readily seen from figures 20 and 23. The above evidence would indicate that the velocity distribution in natural streams is also logarithmic.

A similar rule to that derived above (eq. 47) for open channels can also be obtained for pipes. Bakhmeteff (40) has obtained the following expression for the average velocity defect in a pipe with logarithmic velocity distribution:

$$\frac{U_{max} - \overline{U}}{\sqrt{\frac{\tau_o}{\rho}}} = \frac{3}{2} \frac{1}{k} \tag{48}$$

Introducing equation (48) into (26), and remembering that for pipes d is replaced by r_o, the radius,

$$= \frac{3}{2} \frac{1}{k} = \frac{1}{k} \log_e \frac{y_a}{r_o}$$

and

$$\frac{y_a}{r_o} = e^{-\frac{3}{2}} = 0.224 \qquad (49)$$

where y_a is the distance from the wall of the pipe to the filament moving at the average velocity. The distance y_a is always $.224\ r_o$ and is constant regardless of the roughness or any other condition.

CONCLUSIONS

1. The distribution of the relative concentration of suspended load has the form of the derived distribution law (eq. 29) but does not agree quantitatively with it, i.e., the value of the exponent z given by the theory does not agree with z_1, the exponent that fits the experimental results. When the suspended sediment is fine, z_1 is less than z. This shows that the relative concentration is more uniformly distributed and has a greater average value than that indicated by the theory. In other words, a flow can support and, therefore, transport fine sediment more effectively than the theory indicates. As the size of the sediment is increased, the agreement between the two exponents improves up to a certain point beyond which the value of z may be expected to exceed z_1.

2. The disagreement between the calculated and measured distributions cited under (1), is attributed to the action of the random turbulent fluctuations in suspending sediment. The theory is based on the coefficient for momentum transfer which does not account for the action of the purely random turbulence. Such disagreement was anticipated and the present results confirm it.

3. For fine material the coefficient of sediment-transfer tends to exceed the coefficient of momentum-transfer, while for coarser sediment the opposite tendency is found. The present conclusion, i.e., No. (3), may be considered a corollary of conclusion (1), the physical reason for the conclusions being set forth in (2).

4. Suspended load decreases the coefficient of momentum-

transfer, the reduction varying with the amount of the load and being largest for fine sediment.

5. Suspended load reduces the value of the von Kármán universal constant, k, of turbulent exchange which characterizes the effectiveness of the turbulence in transferring momentum. Reduction of k means that the mixing is less effective and would indicate that the sediment tends to suppress or damp out the turbulence. The present conclusion follows directly from conclusion (4).

6. Suspended load reduces the resistance to flow, thus causing sediment-laden water to flow faster than clear water. (This follows directly from (4) and (5).) In the laboratory channel an average suspended load of 1.2 grams per liter reduced the friction factor, f, as much as 20%, while the Manning roughness coefficient was reduced as much as 10%.

7. The above conclusions (1 to 6, incl.) can all be related to essentially two effects that occur in the flow in the presence of the sediment: (1) the sediment appears to damp out the turbulence in such a way that the momentum-transfer is reduced, and (2) random turbulence, which is not a factor in the transfer of momentum, contributes to the transfer of sediment.

8. Suspended load tends to cause a flow to become unstable and unevenly distributed. Unsymmetrical sediment distribution within the flow may cause secondary circulation.

9. In rivers, density gradients due to suspended load may be an important cause of the secondary circulation that has the effect

of depressing the maximum velocity below the water surface.

10. The velocity distribution near the center of the flume was of the logarithmic form and followed the von Kármán universal velocity defect law.

11. It has been found that the average velocity occurs at about the 0.6 depth in rivers. This velocity can also be determined from the mean of the velocities at depths 0.2 and 0.8. For a logarithmic distribution, the average velocity occurs at depth 0.632, while the mean of the velocities at depths 0.2 and 0.8 is exactly equal to the velocity at depth 0.6. The good agreement on the location of the average velocity in rivers and for logarithmic velocity distribution is taken as evidence that the velocity distribution in rivers follows at least approximately the logarithmic law.

ACKNOWLEDGMENTS

The writer wishes to acknowledge the friendly assistance of professors Theodor von Kármán and Robert T. Knapp and of members of the staff of the Cooperative laboratory. Particular acknowledgment is due Roy Peterson, Milton Wood and Robert Wise for their assistance in collecting and analyzing the data.

The work was carried out with the aid of Work Projects Administration, Official Project No. 65-2-07-58, Work Project No. PS-11496.

APPENDIX I

MEASUREMENT AND CALCULATION OF THE SETTLING VELOCITIES OF THE SEDIMENTS USED AS SUSPENDED LOAD

Settling Velocity of Spheres

Consider a sphere of diameter d_s and density ρ_s settling at its terminal velocity w in a fluid of density ρ and viscosity μ The gravitational force F acting on the particle is given by

$$F = g \frac{\pi d_s^3}{6} (\rho_s - \rho) \quad , \tag{1a}$$

where g is the acceleration of gravity. This force is opposed by a fluid resistance of the same magnitude given by the expression,

$$C_r \frac{\pi d_s^2}{4} \rho \frac{w^2}{2} \quad , \tag{2a}$$

where C_r is a resistance coefficient which is in turn a function, ψ(Re), of the Reynolds number

$$Re = \frac{w d_s}{\frac{\mu}{\rho}} \tag{3a}$$

Equating (1a) and (2a) and rearranging the quantities there follows:

$$C_r \frac{w^2}{g d_s} = \frac{4}{3} \left(\frac{\rho_s}{\rho} - 1 \right) \tag{4a}$$

For very small Reynolds numbers (0 to 0.1), Stokes obtained the

following value for the resistance coefficient:

$$C_r = \psi(Re) = \frac{24}{Re} \qquad (5a)$$

Introducing equations (3a) and (5a) into (4a) and clearing there follows,

$$w = \frac{1}{18}\left(\frac{\rho}{\rho} - 1\right)\frac{1}{\nu} g d_s^2 \qquad (6a)$$

where ν is the kinematic viscosity, $\frac{\mu}{\rho}$, of the fluid. Equation (6a) is known as Stokes law. For higher Reynolds numbers the function, $\psi(Re)$ has been determined experimentally. Figure (1a) shows a plot of the results as summarised by Rouse (36) and can be used to solve equation (4a). It is to be noted that this function is valid for spheres of any density in any fluid.

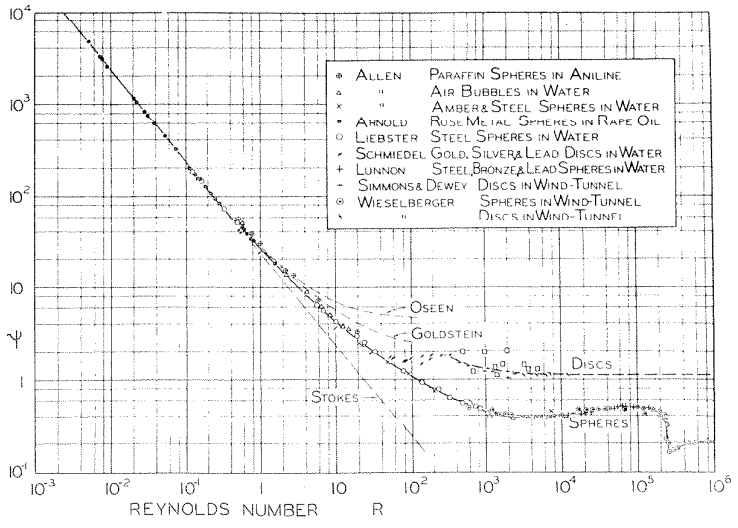

Figure 1a. Plot of Resistance Coefficient of Spheres as a function of Reynolds number

Solutions of equation (4a) with the aid of figure 1a are quite tedious and have been considerably simplified by the use of the chart in figure 2a which was prepared by Rouse. As will be noted, the chart gives the relation between diameter of quartz spheres (ρ_s = 2.65 grams per cc) and their settling velocity in air and water for temperatures ranging from 0 to 40 degrees centigrade.

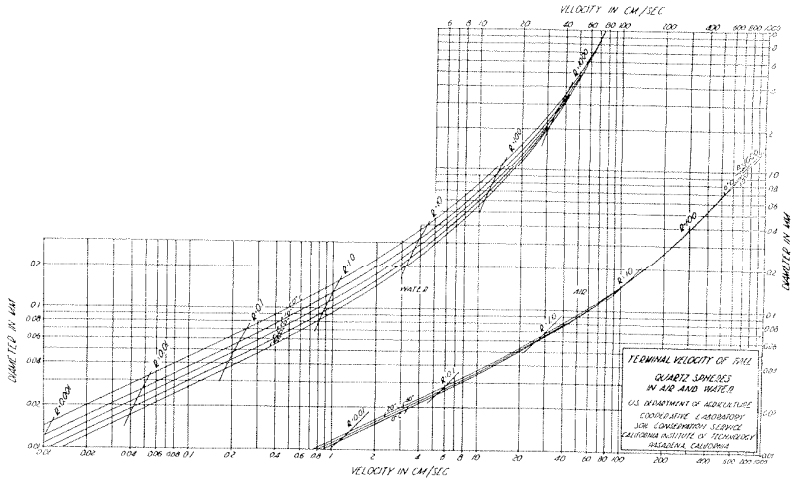

Fig. 2a. Settling velocity of quartz spheres in air and water

Analysis of Direct Settling Velocity Measurements

Consider sediment particles

$$1, 2, 3 \ldots\ldots\ldots n$$

settling in a fluid at terminal velocities

$$w_1, w_2, w_3 \ldots\ldots\ldots w_n$$

The average settling velocity, w_{ave}, of the particles is then,

$$w_{ave} = \frac{1}{n} \sum_{1}^{n} w \qquad (7a)$$

and the geometric mean settling velocity is,

$$w_{g.m.} = (w_1 \cdot w_2 \cdot w_3 \cdot \ldots \cdot w_n)^{\frac{1}{n}} \qquad (8a)$$

The settling velocity $\overline{w}$ of the center of gravity of the group of particles is given by,

$$\overline{w} = \frac{\sum_{o}^{n} w_i m_i}{\sum_{o}^{n} m} \qquad (9a)$$

The sedimentation diameter d_s, of a particle is defined as the diameter of the sphere of the same specific gravity having the same settling velocity as the particle and can be calculated from equation 4a.

Assume now that the mass, m, of a particle is proportional to its sedimentation diameter cubed or,

$$m_i \propto d_{s_i}^3 \qquad (10a)$$

Introducing equation 10a into 9a,

$$\overline{w} = \frac{\sum_{o}^{n} w_i d_{s_i}^3}{\sum_{o}^{n} d_{s_i}^3} \qquad (11a)$$

As a first approximation it is possible to write,

$$w = \overline{w} + (d_s - \overline{d_s}) \left(\frac{dw}{dd_s}\right)_{\overline{w}} , \qquad (12a)$$

where $\overline{d_s}$ is the diameter of the sphere of mass density ρ_s, having settling velocity $\overline{w}$, i.e., having the settling velocity of the center of mass of the group of particles. Introducing equation 12a into 9a gives,

$$\overline{d_s} = \frac{\sum_{o}^{n} m_i d_{s_i}}{\sum_{o}^{n} m} \qquad (13a)$$

Substituting equation 10a into 13a results in,

$$\overline{d_s} = \frac{\sum_{o}^{n} (d_s)^4}{\sum_{o}^{n} (d_s)^3} \qquad (14a)$$

The approximation made in equation 12a is quite good for small ranges of d_s. A close approximation of the range of d_s for the sediments used in the experiments can be obtained from the logarithmic probability plots of the sieve analyses shown in figure 15. For sand III, which is the most poorly sorted, the ratio of the size which is larger than 99.5 percent to that which is smaller than 99.5 percent is 1.9. The geometric standard deviation of the size of this sediment is only 1.13 and indicates that the greatest part (68%) of the material is made up of sizes whose ratio to the mean size is between $1/1.13 = 0.88$ and 1.13. For such a small range in size equation 10a can be expected to give a very close approximation.

Equation 9a was derived by considering individual particles but it also applies to groups of particles where w is the settling velocity of the center of mass of the group and m is its mass. In the same way equations 12a and 13a can be applied to a group of particles. Equations 10a, 11a and 14a can also be applied by merely considering that the group can be represented by the particle with a diameter equal to the average for the group.

Procedure in Measurements and Calculations

As indicated under "Procedure" the settling velocity $\overline{w}$, and

sedimentation diameter $\overline{d_s}$, were determined for the material retained on each sieve of the standard set ~~of sieves~~, and these results were then used to determine the sedimentation diameter of a sediment composed of several sieve fractions.

Small samples (30 to 75 grains) of each sieve fraction were taken, and the time for individual grains to settle a given distance in tap water was measured. The settling column was a liter graduate (diameter 2-3/8 in.) which was filled with tap water having the same temperature as the room. In general the measurements were made during a time when the changes in room temperature were small. The temperatures were measured with an immersion thermometer reading to 0.1 degree centigrade.

The geometric mean settling velocity $w_{gm.}$, (eq. 8a) and the corresponding sedimentation diameter were determined by arithmetic computation, and the sedimentation diameter, $\overline{d_s}$, of the center of mass of the particles was calculated from equation 14a. To reduce the work involved in this calculation, particles were grouped into a number of convenient classes according to settling times and the average diameter for each class weighted according to equation 14a to give $\overline{d_s}$.

Table Ia gives the results of these settling velocity measurements along with other pertinent data. Figure 3a shows a plot of the sedimentation diameters shown in table Ia against the average sieve opening, i.e., average of openings of sieve retaining material and of sieve through which material passed. The plot shows clearly that the mean sedimentation diameter is larger than the average sieve opening.

TABLE Ia

Results of Settling Velocity Measurements for Silica Sand in Water

Sieve opening mm.			No. of Particles in Sample	Temperature Deg. Cent.		Geom. Mean Settling Vel. Wgm	$\frac{d_s}{d_m}$	Sedimentation diameter- mm.			
Sieve Above	Sieve Retain. Sed.	d_m		Min.	Max.			Corresponding to Wgm		$\overline{d_s}$	
								Sample	Ave.	Sample	Ave.
.208	.175	.191	47	15.6	16.5	2.21	1.04	.196	.194	.202	.198
			67	21.8	22.1	2.36		.192		.194	
.175	.147	.161	51	14.8	15.1	1.58	1.04	.161	.164	.166	.168
			58	17.2	17.7	1.75		.167		.170	
.147	.124	.135	72	18.3	18.8	1.51	1.13	.151	.150	.152	.153
			50	15.6	15.8	1.42		.150		.155	
.124	.104	.114	51	17.1	18.3	1.12	1.13	.127	.126	.132	.129
			43	18.4	19.4	1.13		.126		.127	
.104	.088	.096	35	21.8	23.4	0.84	1.11	.098	.104	.105	.107
			56	23.5	25.0	0.915		.104		.105	
			68	25.0	26.0	0.972		.105		.110	
			29	27.2	27.4	1.05		.110		.110	
.088	.074	.081	35	27.4	27.6	0.831	1.19	.095	.092	.098	.096
			40	25.5	25.9	0.776		.092		.096	
			34	26.0	26.8	0.775		.092		.094	
			49	26.9	27.5	0.775		.091		.095	
.074	.061	.068	68	27.8	28.5	0.703	1.26	.085	.084	.090	.086
			49	29.2	29.4	0.713		.085		.086	
			49	29.8	30.0	0.839		.078		.081	
			34	31.5	31.7	0.764		.086		.086	

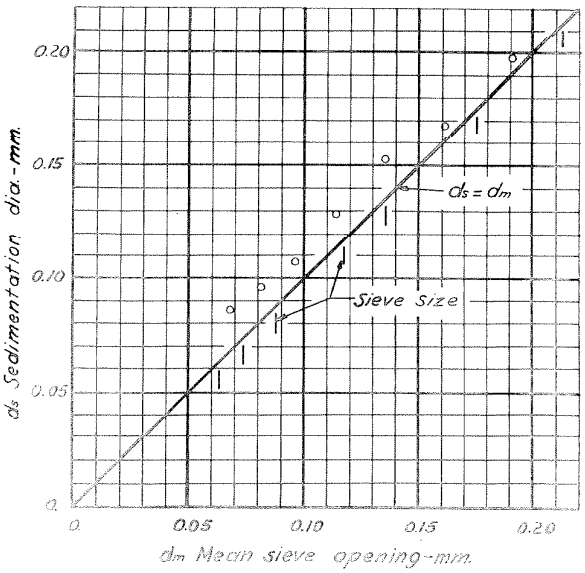

Fig. 3a. Plot of Mean sedimentation Diameter Against Mean Sieve Opening

The sieve analysis gives the percent by weight P, of the material held on each sieve. Table Ia gives the sedimentation diameter of each sieve fraction which, along with the weight, makes possible the calculation of $\overline{d_s}$ for the sample by using equation 3a. In this case each fraction can be considered as having a mass which is P percent of the total mass M of the sample. Equation 13a then becomes,

$$\overline{d_s} = \frac{\sum_{o}^{n} P_i d_{s_i}}{100} \qquad (15a)$$

Table IIa shows the application of equation 15a to the calculation of the sedimentation diameter of sand I whose sieve analysis is shown in figure 15.

TABLE IIa

Calculation of Sedimentation Diameter of sand I from Sieve Analysis.

Sieve opening mm.	Percent Passing	Percent retained (P)	Sedimentation diameter d_s mm.	P x d_s
.246	99.99	0.01	.270	.003
.208	99.96	0.03	.227	.007
.175	97.34	2.62	.198	.520
.147	46.35	50.99	.168	8.566
.124	5.89	40.46	.153	6.191
.104	0.13	5.76	.129	.746
.088	0.08	0.05	.107	.005
.074	0.05	0.03	.096	.003
				$\sum$ = 16.044
				d_s = .160 mm

The sedimentation diameters for the sieves with openings of .208 mm and .246 mm were estimated from figure 3a. The effect of any error in this estimate is obviously negligible for the above calcula-

tion since the weight percentages for this size are quite small.

In order to check the calculation of the mean sedimentation diameter illustrated by table IIa, direct settling velocity measurements were made of samples of the complete sediment. The settling-time measurements as well as the calculations to obtain $\overline{d_s}$ were made in the manner outlined for the sieve fractions. The results of such measurements on 2 samples of sand I and 3 samples of sand II are shown in table IIIa and indicate very good agreement between the two methods of determining the mean sedimentation diameter $\overline{d_s}$.

TABLE IIIa

Comparison of sedimentation diameters obtained from direct settling velocity measurements and from sieve analyses by the method illustrated in table IIa.

Sand	From direct settling velocity measurements				$\overline{d_s}$ - mm from sieve analysis
	Sample No.	No. of Grains	$\overline{d_s}$ - mm. Sample	$\overline{d_s}$ - mm. Ave.	
I	1	257	0.161	0.160	0.160
	2	130	0.160		
II	3	69	0.131	0.132	0.133
	4	90	0.132		
	5	80	0.132		

Figure 4a shows a logarithmic probability plot of the settling velocity for sample 1 of table IIIa. The abcissa scale is laid out geometrically so velocities one space apart are in the ratio of $\sqrt[8]{2}$. The ordinate values are the percentages of the total number of particles

whose settling velocity is less than the corresponding abcissa value.

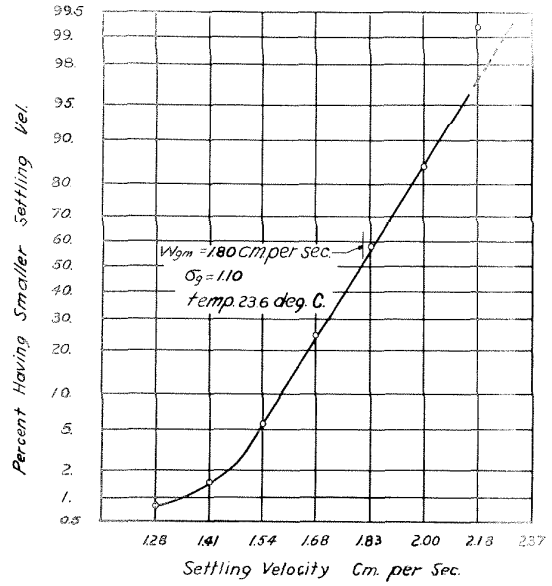

Fig. 4a. Logarithmic probability plot of settling velocity distribution for sand sample 1, table IIIa.

The straight line plot on the figure shows that the distribution of settling velocities follows the normal error law and substantiates the statement by Otto and Rouse (34) that the air classifier used to prepare the sediment actually sorts material according to its settling velocity. The plot of the sieve analysis of this same sand in figure 15 shows that the distribution of sieve diameters is also very close

to the normal error law.

The value of the geometric mean settling velocity $w_{g.m.}$, read directly from figure 4a is 1.80 cm/sec. This value is identical with that obtained from equation 8a. The value of the geometric standard deviation, $\sigma_g = 1.10$, read from the curve is the ratio of the velocity at the ordinate value of 84.1% to the geometric mean velocity, or the ratio of the geometric mean velocity to the velocity at the ordinate value of 15.9%. Or in other words, the ratio of the extreme settling velocities of the central 68% of the particles is 1.10 x 1.10 = 1.21. Incidentally, the value of σ_g calculated from the numerical data was 1.11 while σ_g for the sieve analysis, figure 15, is 1.14.

The good agreement of the settling velocity measurements can be taken as a justification of the assumptions made in the analysis and as an indication of the uniformity of the technique. The absolute accuracy of the results is of course determined by the accuracy of the original settling time measurements on individual grains. The most likely source of error arises from temperature gradients within the fluid of the settling column, which in turn give rise to density currents or convection currents. In general, the temperatures were rising during the measurements and one would then expect the outer layers of the fluid in the column to be warmer and therefore lighter than the center. This would give rise to convection currents going downward in the center, where the particles were settling, and upward at the cylinder wall and would increase the apparent settling velocity and hence the sedimentation diameter of the sediment. If such con-

vection currents do exist, one would expect their influence to decrease as the actual settling velocity of the sediment became larger. A close inspection of Figure 3a shows that the sedimentation diameter approaches more closely to the sieve diameter as the particles increase in size and might be taken as proof of the existence of convection currents. The work of Knapp (37), who found that for subsieve material the sedimentation diameter was about 4% smaller than the sieve size, also leads to a similar conclusion. However the above results are in close agreement with settling velocity measurements made by Rouse (26) in a 12 inch diameter glass jar.

Although the above discussion indicates the possibility of errors in the settling velocity measurements, it is felt that further investigation is necessary before further conclusions can be made. It is also felt that any errors that do exist are small.

BIBLIOGRAPHY

1. Kennedy, R. G.: Hydraulic Diagram for Canals in Earth. Minutes of Proceedings, Inst. Civ. Engrs., Vol. 119, p 281, 1895

2. Lane, E. W.: Stable Channels in Erodible Material. Trans. Am. Soc. Civ. Engrs., Vol. 109, p 123, 1937.

3. Griffiths, W. M.: A Theory of Silt Transportation, Trans. Am. Soc. Civ. Engrs., Vol. 104, p 1733, 1939.

4. Krey, H.: Zentralblatt d. Bauverwaltung. Nos. 39-40, 1919.

5. Wattendorf, F. W.: Investigations of Velocity Fluctuations in a Turbulent Flow. Jour. Aero. Sci., Vol. 3, pp 200-202, 1936.

6. Reynolds, O.: Phil. Trans. Roy. Soc. 1895.

7. Prandtl, L.: The Mechanics of Viscous Fluids. Aerodynamics Theory, Julius Springer, Vol. III, p 125, 1935.

8. Boussinesq, Joseph,: T. V. Mem. pres. par. div. Sav., Vol. XXIII, Paris, 1897-1977. Theorie des l'ecoulement tourbillonnant.

10. Prandtl, L.: Bericht über Untersuchungen zur ausgebildeten Turbulenz. Z f. angew. Math. Mech., Vol. 5, No. 2, p 136, 1925.

11. von Kármán, Th.: Some Aspects of the Turbulence Problem. Proc. 4th Int. Cong. Applied Mech., Cambridge, England, 1934.

12. Schmidt, Wilhelm,: Der Massenaustausch in freier Luft und verwandte Erschsinungen. Probleme der kosmischen Physik, Band 7, Hamburg, 1925.

13. O'Brien, M. P.: Review of the Theory of Turbulent Flow and its Relation to Sediment-transportation. Trans. Am. Geophys. Union, pp 487-491, April 27-29, 1933.

15. Leighly, John B.: Toward a Theory of the Morphologic Significance of Turbulence in the Flow of Water in Streams. Univ. of California Publ. in Geography, Vol. 6, No. 1, pp 1-22. Berkeley, 1932.

16. DuBoys, P.: Annales des ponts et chaussees, Series 5, Vol. 18, pp 149-195. 1879.

17. von Kármán, Th.: Turbulence and Skin Friction. Jour. Aero. Sic., p 1, Vol. 1, No. 1, Jan. 1934.

18. Nikuradse, J.: Gesetzmaessigkeiten der turbulenten Strömung in Glatten Rohren. V.D.I. Forschungsheft 356, 1932.

19. Nikuradse, J.: Stroemungsgesetze in Rauhen Rohren. V.D.I., Forschungsheft, p 22, Vol. 4. 1933.

20. Keulegan, Garbis H.: Laws of Turbulent Flow in Open Channels. Jour. of Research, U. S. Dept. of Commerce - National Bureau of Standards, Vol. 21, pp 707-741. Dec. 1938.

21. Rouse, Hunter: Modern Conceptions of the Mechanics of Fluid Turbulence. Trans. Am. Soc. Civ. Engrs., Vol. 102, p 463, 1937.

22. Rouse, Hunter: An Analysis of Sediment Transportation in the Light of Fluid Turbulence. U. S. Dept. Agri. Mimeograph Publ. SCS-TP-25, July 1939.

23. Lane, E. W. and Kalinske, A. A.: The Relation of Suspended Load to Bed Material in Rivers. Trans. Am. Geophys. Union, Part IV, p 637, 1939.

24. Knapp, Robt. T.: Energy Balance in Stream Flows Carrying Suspended Load. Trans. Am. Geophys. Union, Section of Hydrology, 1938.

25. Hurst, H. E.: The Suspension of sand in Water, Proc. Royal Soc. A. Vol.124, pp 196-201, 1929.

26. Rouse, Hunter: Experiments on the Mechanics of Sediment Suspension. Proc. Fifth Int. Cong. Applied Mech., p 55, 1938.

27. Leighly, John B.: Turbulence and the Transportation of Rock Debris by Streams. Geographical Review, Vol. XXIV, No. 3, pp 453-464. New York, July, 1934.

28. Christiansen, J. E.: Distribution of Silt in Open Channels. Trans. Am. Geophys. Union, Part II, p 478, 1935.

29. Fortier, Samuel, and Blaney, H.: Silt in the Colorado River and its Relation to Irrigation. U. S. Dept. Agriculture, Technical Bulletin 67.

30. Richardson, E. G.: The Transportation of Silt by a Stream. Phil. Mag., Vol. 17, pp 769-783. 1934.

31. Richardson, E. G.: The Suspension of Solids in a Turbulent Stream. Proc. Roy. Soc. A. Vol. 162, p 583, 1937.

32. Oaks, Robert M. & Knapp, Robt. T.: A "Closed-circuit" Flume for Suspended-Load Studies. Trans. Am. Geophys. Union, Part II, p 525, 1936.

33. Peters, H.: Pressure Measurement: Handbuch der Experimentalphysik, Vol. IV, Part 1, L. Schiller, Leipzig.

34. Otto, George H. and Rouse, Hunter: Wind-tunnel Classifier for Sand and Silt. Civ. Engr., Vol. 9, No. 7, July 1939.

35. Otto, George H.: A Modified Logarithmic Probability Graph for the Interpretation of Mechanical Analyses of Sediments. Jour. Sed. Pet., August, 1939.

36. Rouse, Hunter: Nomogram for the Settling Velocity of Spheres. Exhibit D of the Report of the Committee on Sedimentation, pp 57-64. Oct. 1936-37.

37. Knapp, Robert T.: New Apparatus for Determination of Size Distribution of Particles in Fine Powders. Ind. & Eng. Chem., Vol. 6, p 66, Jan. 15, 1934.

38. Buckley, A. B.: The Influence of Silt on the Velocity of Water Flowing in Open Channels. Min. Proc. of Inst. of Civ. Engrs., Vol. 216, p 183, 1922-1923.

39. Giandotti, Prof. Ing. Mario: Les Deplacements du Lit du Po, Le Service Hydrographique Italien. XV Congress International de Navigation, Venice, Sept. 1931.

40. Bakhmeteff, Boris H.: The Mechanics of Turbulent Flow. Princeton University Press. 1936.

SYMBOLS

A = Area of cross section of stream

a = Reference level for suspended-load distribution function

β = Correlation coefficient

β_1 = " "

c = Constant coefficient

c_1 = " "

c_s = Specific heat

C = Concentration of suspended load

C_a = Concentration of suspended load at reference level

C_m = Mean value of concentration over cross section

$\overline{C}$ = Average value of concentration over profile

γ = Specific weight of fluid

d = Depth of water

d_s = Sedimentation diameter of sediment

$\overline{d_s}$ = Mean value of d_s

d_m = Geometric mean sieve size

δ = Small distance

ϵ = Mixing coefficient

F = Force

f = Friction factor for pipes

G_1 = Sediment load

g = Acceleration of gravity

g_h = Rate of transfer of heat

E = Suspended-load distribution function

k = Universal constant

k_s = Height of roughness element

l = Mixing length

m = Mass

μ = Coefficient of viscosity

n = Manning roughness coefficient

n = Constant exponent

n = Number of particles per unit volume

$\nu = \frac{\mu}{\rho}$ Kinematic viscosity

p = Wetted perimeter of cross section

q = Rate of discharge, volume per unit time

R = Hydraulic radius of section

Re = Reynolds number

r_o = Radius of pipe

ρ = Density of fluid. Mass per unit volume

ρ_s = Density of sediment. Mass per unit volume

S = Slope of bottom of channel

σ_g = Geometric standard deviation

τ = Shearing stress at any point

τ_o = Shearing stress at boundary

θ = Temperature

U = Mean velocity in horizontal or x direction

$\overline{U}$ = q/A Average velocity at cross section

U_1 = Average velocity at profile

U_{max} = Maximum velocity at profile

U' = Turbulent fluctuation parallel to U

U_s = Velocity at entrance to sampler tip

V = Velocity

V' = Turbulent fluctuation normal to U

w = Settling velocity of particle

w_{gm} = Geometric mean settling velocity of sediment

$\overline{w}$ = Settling velocity of center of mass of a group of particles

$z = \dfrac{w}{k\sqrt{\frac{\tau_o}{\rho}}}$ = exponent for suspended-load distribution function (given by theory).

z_1 = Exponent for suspended-load distribution function that fits data. (experimental value)